

Review

# Polymer-Based Coating for Steel Protection, Highlighting Metal–Organic Framework as Functional Actives: A Review

Sarah Bill Ulaeto <sup>1,2,3,\*</sup> , Rajimol Puthenpurackal Ravi <sup>2,3</sup>, Inime Ime Udoh <sup>4</sup> , Gincy Marina Mathew <sup>5</sup>  
and Thazhivilai Ponnu Devaraj Rajan <sup>2,3,\*</sup>

<sup>1</sup> Department of Chemical Sciences, Rhema University Nigeria, Aba 453115, Nigeria

<sup>2</sup> Material Science & Technology Division, CSIR-National Institute for Interdisciplinary Science and Technology, Trivandrum 695019, India; rajipr19@gmail.com

<sup>3</sup> Academy of Scientific & Innovative Research (AcSIR), Ghaziabad 201002, India

<sup>4</sup> School of Environmental and Chemical Engineering, Shenyang Ligong University, Shenyang 110159, China; udoh15b@alum.imr.ac.cn

<sup>5</sup> Microbial Processing & Technology Division, CSIR-National Institute for Interdisciplinary Science and Technology, Trivandrum 695019, India; gincymarina@gmail.com

\* Correspondence: sarahbillmails@yahoo.com (S.B.U.); tpdrajan@niist.res.in (T.P.D.R.)

**Abstract:** Polymer-based coatings are a long-established category of protective coatings for metals and alloys regarding corrosion inhibition. The polymer films can degrade, and when coated on metallic substrates, the degradation facilitates moisture and oxygen penetration, reducing the polymer film's adhesion to the metallic substrate and exposing the substrate to extreme conditions capable of corrosion. For this reason, pigments, inhibitors, and other compatible blends are added to the polymer coating formulations to enhance adhesion and protection. To prevent the possible deterioration of inhibitor-spiked polymer coatings, inhibitors are encapsulated through diverse techniques to avoid leakage and to provide a controlled release in response to the corrosion trigger. This review discusses polymer-based coating performance in corrosion-causing environments to protect metals, focusing more on commercial steels, a readily available construction-relevant material used in extensive applications. It further beams a searchlight on advances made on polymer-based coatings that employ metal–organic frameworks (MOFs) as functional additives. MOFs possess a tailorable structure of metal ions and organic linkers and have a large loading capacity, which is crucial for corrosion inhibitor delivery. Results from reviewed works show that polymer-based coatings provide barrier protection against the ingress of corrosive species and offer the chance to add several functions to coatings, further enhancing their anti-corrosion properties.

**Keywords:** polymer-based coating; corrosion inhibition; encapsulation; controlled release; steel; metal–organic framework; functional additives



**Citation:** Ulaeto, S.B.; Ravi, R.P.; Udoh, I.I.; Mathew, G.M.; Rajan, T.P.D. Polymer-Based Coating for Steel Protection, Highlighting Metal–Organic Framework as Functional Actives: A Review. *Corros. Mater. Degrad.* **2023**, *4*, 284–316. <https://doi.org/10.3390/cmd4020015>

Academic Editors: Viswanathan S. Saji and Mikhail Zheludkevich

Received: 31 May 2022

Revised: 17 April 2023

Accepted: 21 April 2023

Published: 29 April 2023



**Copyright:** © 2023 by the authors. Licensee MDPI, Basel, Switzerland. This article is an open access article distributed under the terms and conditions of the Creative Commons Attribution (CC BY) license (<https://creativecommons.org/licenses/by/4.0/>).

## 1. Introduction

Coatings are multi-layered systems that include a primer and topcoat. Each layer is responsible for certain specified functions depending on what the film is designed to achieve. The layered coating system results in a robust function for the underlying substrate. The interactions and interfacial phenomenon control the general performance of multi-coating systems [1]. Surface film properties are typically related to the specific components of the coating system [2]. These substrate coverage materials can be formulated to provide a combination of protective and decorative purposes.

Coatings intended for metal protection against hostile environments must primarily proffer physical barriers effective enough to impede deterioration of the exposed surfaces when in contact with aggressive species [3]. However, protective coatings encounter complex destructive factors. These range from mechanical action to physicochemical action to microbiologically influenced factors during service [4]. Polymer coatings are known

to protect substrates and surfaces, whether ferrous or non-ferrous. These polymers are macromolecules, usually of high molecular weight, capable of covering a large area of the exposed surface. Polymers offer substantial coverage in diverse media, such as acidic, basic, and neutral media. The excellent film-forming properties of polymers and their adhesive properties have strongly supported the use of polymers in the corrosion protection of metal substrates. The flexibility of polymers also allows their mixture with other compounds and additives to improve pore-sealing effects, limit the ingress of deteriorating species, and inhibit the degradability of the polymeric film formed [5]. A wide range of additives can be used in the fabrication of polymer-based coating, including metal-organic frameworks (MOFs), graphene oxide (GO), and oxides of iron, silicon, titanium, etc. However, while we acknowledge the use of other additives, a detailed discussion on using MOF as a typical additive in polymer-based coating is given in Section 4. Polymer-based coatings are relevant and in high demand due to their unique characteristics such as toughness, antimicrobial, corrosion resistance, high tensile strength and resilience, and non-conductivity to heat and electricity [6].

The properties of MOFs put them among the attractive additives in polymer-based coatings. With porous microstructures, MOFs have attracted widespread synthesis and use in recent years. They have found applications in storing gas and energy, separation, sensing, environmental science, technology, and even medicine. However, their effectiveness in anti-corrosion coatings has also received notice. The effective delivery of corrosion inhibitors for anti-corrosion purposes requires materials with a high loading capacity, such as MOFs. These MOFs are popular among micro- and nano-porous materials with a tailorable structure of metal ions and organic linkers [7,8]. Recently, coatings made from several MOFs (such as UiO-66, MIL-53, and ZIF-8) have successfully been engineered to exhibit good corrosion prevention performance and water stability [9]. MOFs can be made more adaptable to microstructural changes than other porous nanoparticles by adjusting the kind and quantity of metal ions and the organic linkers [10]. MOFs can be produced synthetically in various shapes, including triangular, square, planar, and linear shapes. Inorganic components for MOF structures can include di-, tri-, and tetravalent metal ions [11,12]. Literature search reveals that the fabrication strategy for a bulk of MOFs with varied architectures and topologies typically adopts conventional solvothermal and non-solvothermal techniques [13]. Moreover, producing structurally optimized MOFs for high-tech applications is possible by carefully selecting suitable metal ions and organic ligands [14,15]. The application of MOF-based corrosion protection materials also faces several issues, such as weak durability, unstable protection performance, and poor adhesion, despite numerous studies proving that MOFs exhibit good anti-corrosion capabilities [9]. This review also attempts to highlight recent applications of MOFs in polymer-based coating for the corrosion protection of steel.

Carbon steel, commonly referred to as just “steel”, is a readily available construction-relevant material used in extensive applications. Mild steel is one of the largest groups of carbon steel in everyday use. The cost-effective machinable substrate makes it a choice material for research and real-time service applications. However, it is highly prone to corrosion with the slightest exposure. This shortcoming has resulted in several industrial accidents that can be controlled by applying protective coatings such as polymer-based coatings. Mild steel is produced in different conditions, allowing for categorizing it as either hot-rolled, cold-rolled, or galvanized steel based on the finishing method during its processing.

Upon exposure of steel to moisture, corrosion results in rust formation because steels consist mainly of iron. Iron oxidizes rapidly on exposure to the atmosphere, and the electrons reduce oxygen in the air (Equations (1)–(3)). Iron (II) ions in Equation (3) further react with atmospheric oxygen, and the result is rust, a hydrated iron (III) oxide (Equation (4)). The rusty layer is not protective but usually flakes off, exposing the underlying iron to further corrosion by continuous deterioration, gradually thinning and weakening the

substrate. Figure 1 shows a schematic illustration of steel coupon, coated steel, and the deteriorating effect of corrosion on steel.

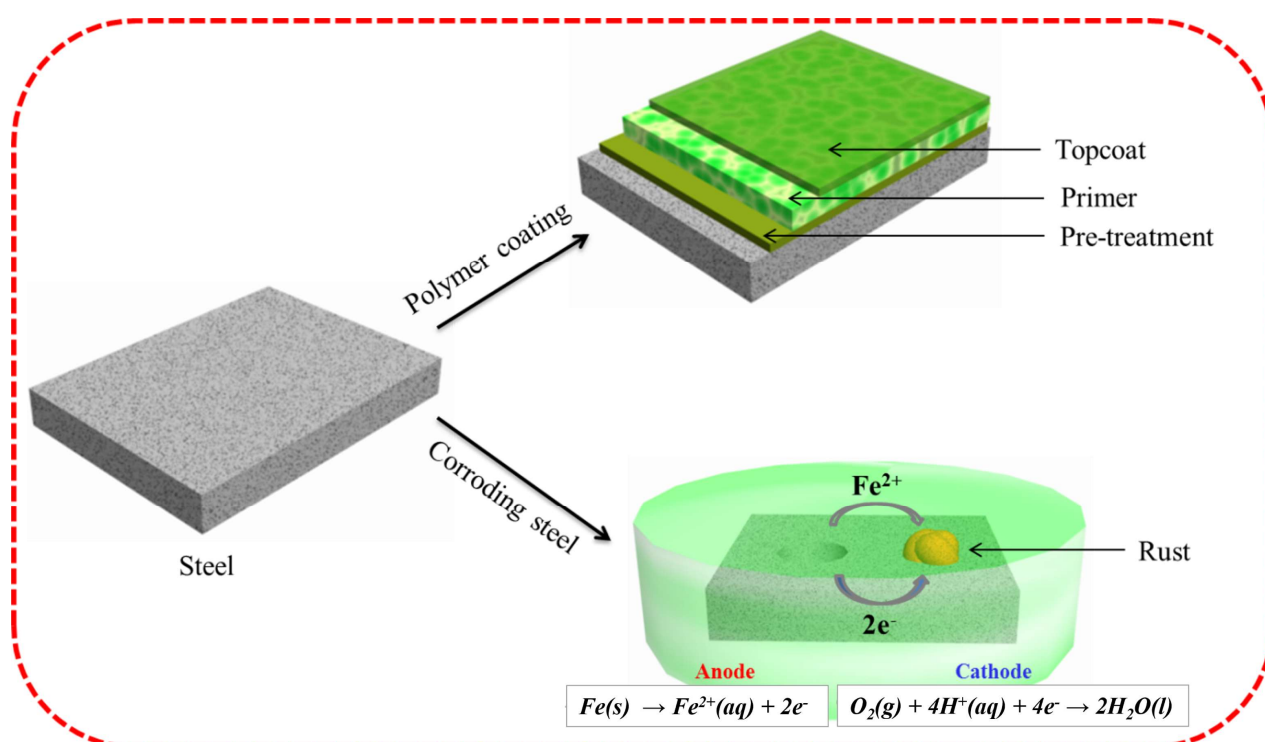
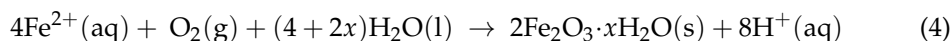
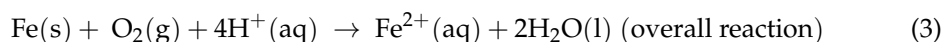
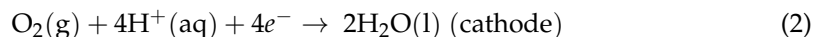
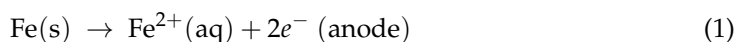


**Figure 1.** Schematic representation of pristine steel coupon, coated steel, and the deteriorating effect of corrosion on steel in a corrosive environment.

Herein, this review discusses various polymer-based coating systems used for corrosion prevention and later focuses on applying MOFs as an example of a functional additive in polymer-based coatings in corrosion prevention techniques. A detailed account of different polymers, commonly used fillers for the polymer, other corrosion detection techniques used, and the efficiency of each system is given in detail but in an exact manner. The synthesis of MOFs is discussed to provide insight into this class of materials capable of delivering active corrosion protection in polymer-based coating. Aside from efficiency, some minor practical limitations and challenges faced during the application and the methods to rectify these limitations are also given in this review. The mechanism of action of MOF as functional additives is described in addition to other outlined inhibiting additives in polymer-based coatings when considering the future direction of polymer-loaded anti-corrosive coatings. Other reviews focused solely on MOFs applicable in diverse forms and their recent innovations for corrosion protection.

## 2. Categories of Polymer-Based Coatings

Over time, a wide range of polymeric materials has become vital components of coatings for preservation and aesthetics. The flexible nature of polymers has also allowed

the incorporation of other materials to enhance the performance of coatings. In this discourse, the polymer coatings are categorized as shown in Figure 2 to provide a scope for this work.

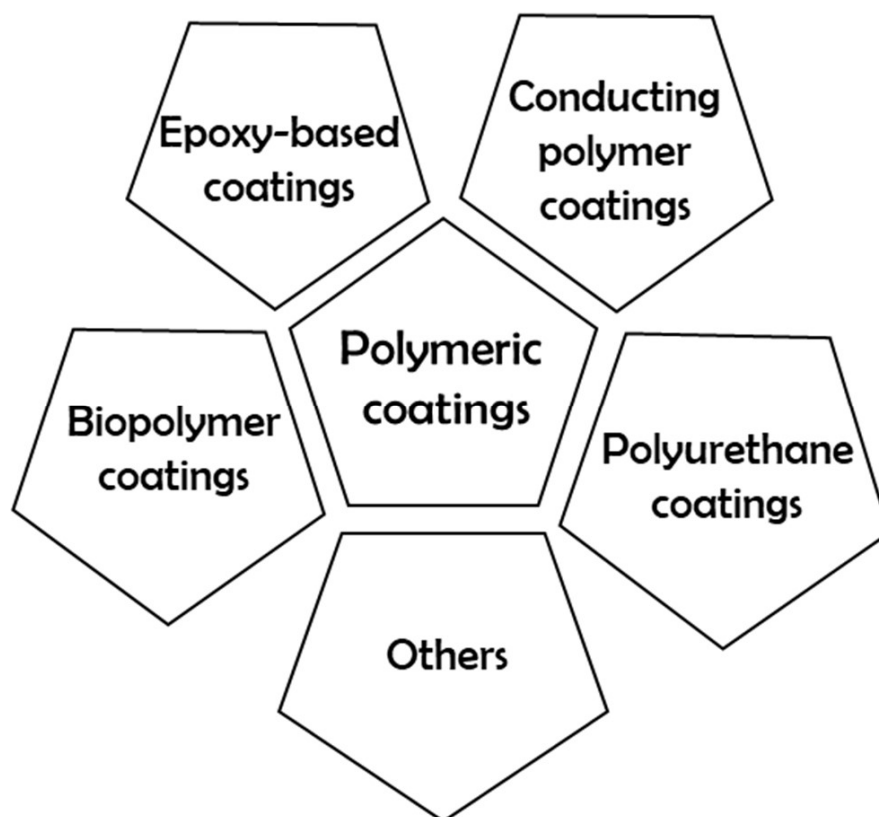


**Figure 2.** Polymeric coatings for the preservation of substrates and surfaces.

### 2.1. Conducting Polymer Coatings

Conducting polymers is of great interest due to their electrochemical and mixed ionic/electronic conductivity properties [16]. They are widely used as host matrices to fabricate various composite films. Particles incorporated into conducting polymers modify specific parameters like morphology, conductivity, and physical properties. The particle may be either inorganic or organic depending upon the final application requirement, for instance, corrosion protection. The presence of conductive polymers in some polycrystalline nanocomposites displayed novel properties. Also, in various paints, low concentrations of nano-particulate dispersions of organic metal polyanilines (PANI) resulted in remarkable effects in corrosion protection [17]. Goswami et al. [18] fabricated several structural forms of polyaniline (PANI) and corresponding nanocomposites with graphene as functional fillers for the epoxy coating to reduce mild steel corrosion. The interfacial wrapping of the graphene skeleton by PANI was made more accessible by the  $\pi$ - $\pi$  interactions between the aromatic rings of in situ generated, covalently bonded PANI on p-phenylenediamine functionalized graphene (fGO). When compared to the emerald base form of PANI (PANI-EB), the emerald salt form (PANI-ES) had a noticeably greater impedance and improved corrosion prevention capabilities, as revealed by the Nyquist and Bode plots in Figure 3. Moreover, the anti-corrosive capabilities of PANI were significantly enhanced by the graphene skeleton in the fGO-PANI nanocomposite, which resulted in a further increase in total impedance.

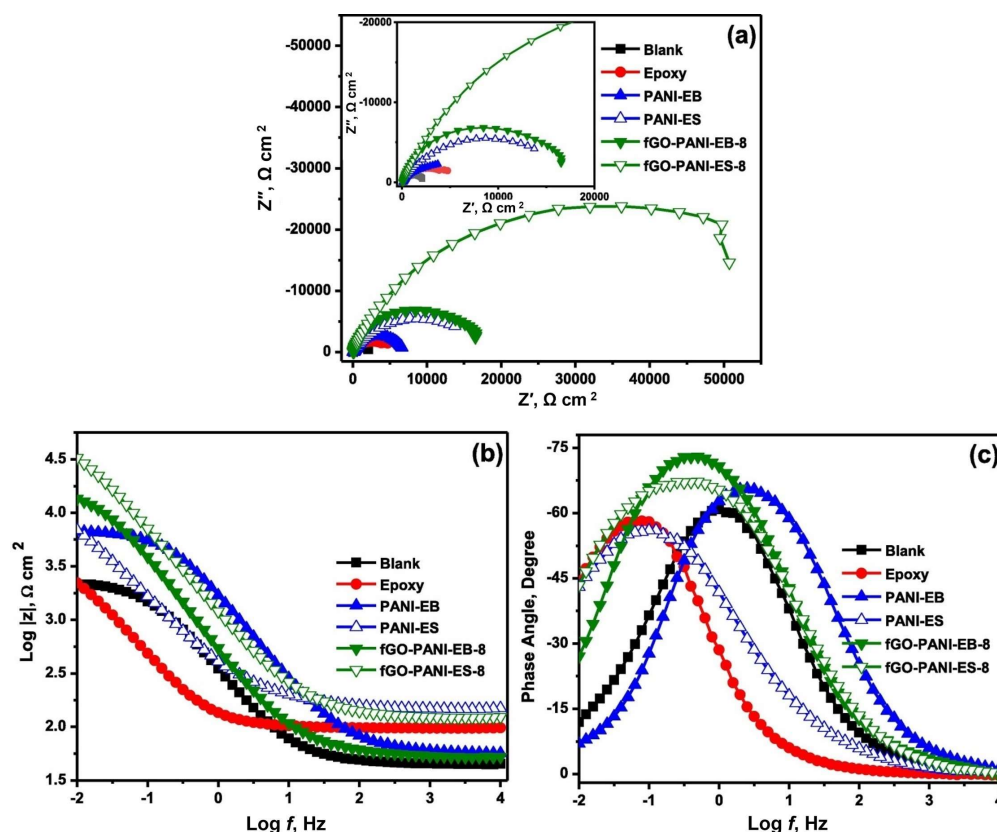


**Figure 3.** (a) Nyquist and (b,c) Bode plots of uncoated mild steel (blank) and coated samples (epoxy, PANI-EB, PANI-ES, fGO-PANI-EB-8, and fGO-PANI-ES-8) after exposure to 3.5% NaCl solution. Reproduced with permission [18], copyright 2022, Elsevier.

Melt dispersion of polyaniline produces fine particles which self-organize into complex ultrafine networks. Apart from polyaniline, other nano-conducting polymers such as polythiophene and polypyrrole enhance corrosion resistance when used. Incorporating strong oxidizing species into a polymer resin is expected to enhance the oxidizing power of the polymers. The presence of oxides such as  $\text{Fe}_3\text{O}_4$  in polypyrrole nanocomposites has prospects for use in the corrosion protection of iron [19]. Yeh and Chin reported that clay containing polypyrrole nanocomposites provided better corrosion protection than the unmodified polypyrrole resin [20].

## 2.2. Polyurethane Coatings

Polyurethanes are versatile polymers containing polyol and isocyanate precursors. Their outstanding mechanical, physical, and chemical properties have increased their demand as industrial coatings materials. Polyurethane applications manufacture paints and adhesives, footwear and car parts, foams, insulating plates, etc. [21,22]. In coatings fabrication, solvent, and water-borne polyurethanes can be utilized. However, solvent-based polyurethanes are strongly relevant in fibers and coatings, adhesives, foams, and elastomer applications due to their resistance to chemicals, water, and other solvents. Their flexibility, adhesion to a broad range of substrates, and abrasion resistance strongly contribute to their relevance. However, the evaporation of volatile organic compounds is part of its environmental concerns. Thus, versatile, eco-friendly water-borne polyurethanes are preferred, even though rapid microcrack propagation upon physical damage is challenging following their use [23]. The applications of polyurethane coatings in the industry are attributed to several factors, such as extensive mechanical strength, resistance to scratch, corrosion, chemicals, and low-temperature flexibility [24]. Bio-derived polyurethane coatings have been widely investigated. An example is scratch-free surface coatings using chitosan-based



polyurethane coatings. When scratched, the damage formed on the surface of the chitosan layer can be healed using a UV component in the sunlight [25]. Polyurethane coatings from neem oil polyester amides have shown promising effects in protecting mild steel from rusting [26]. The evidence of the anti-corrosive performance of polyurethane coating of different percent composition during immersion in 3.5 wt.% NaCl solution is shown in Figure 4. In addition, neem acetylated polyester polyol [27] has been investigated and holds great promise for protecting mild steel against corrosion.

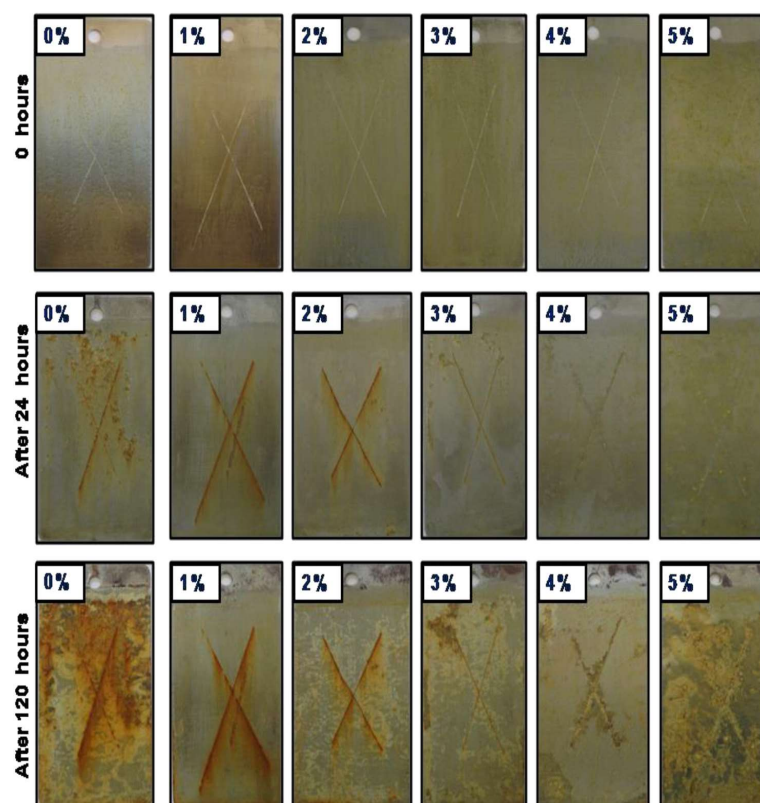


**Figure 4.** Immersion test images of polyurethane coatings exposed to 3.5 wt.% NaCl solution. Reproduced with permission [26], copyright 2013, American Chemical Society.

### 2.3. Epoxy-Based Coatings

Epoxy coatings are derived from thermoset epoxy resins known for their extensive application as protective films for structural and specialty metallic materials. Epoxy resins are widely modifiable, solvent-free, or solvent-based matrices. The epoxy technology cuts across diverse sectors, including aerospace, manufacturing, automobile, and household goods, to mention a few, either as films or composites. Solvent-based epoxy coatings are low-cost and provide excellent chemical resistance, adhesion to metallic substrates, exceptional processability, etc. [28]. Epoxy resins can be synthesized in many ways with varying cure times. The curing agents could be nitrogen, oxygen, sulfur-containing compounds, amine-boron trihalide complexes, cationic salts, or quaternary phosphonium salts [29]. Production of epoxy resins from the reacting bisphenol A with epichlorohydrin dates back to the 1930s. Since that time, epoxy resins have been used for coatings and castings. They are also regularly used for potting, adhesives, binders, and encapsulates. The classes of widespread use and commercialized epoxies are aromatic glycidyl amines, cycloaliphatics, and phenolic glycidyl ethers [30].

Commercialized epoxy resins under different trade names are based on their form (solid, liquid, or semi-solid), viscosity, equivalent weight, and the number of reactive sites per molecule [30,31]. Commercially available epoxies commonly used for coating purposes include Epon 828, DER 661, MY 720, CY 179 [30]; Epon 1001 [28]; GY 250 [32]; E44 [33,34];

KER 828 [35]; E-20-75 [36]; WSR6101 [37], etc. Commercialized curing agents with different brand names include Epikure [31], CRAYAMID 140C [35], D-3282 [38], Versamid 115 [39], HY 951 [32], Anquamine 615 [37], etc. These curing agents could contain amines or amides such as diethylenetriamine (DETA), triethylenetetramine (TETA), polyamides, aromatic amines, etc., and differ with curing temperature. However, the degree of curing of these two-part epoxy systems depends on the epoxy-to-hardener ratio. This ratio also influences thermal and mechanical properties. Epoxy resins are usually used as primer coatings [36] and rarely as topcoats due to their known shortcoming of exposure to UV light. To achieve UV light stability for coating, titanium dioxide ( $\text{TiO}_2$ ) can be added to the epoxy formulation [40]. Other nanofillers can be employed for better protection. For example, titanium oxide-graphene oxide ( $\text{TiO}_2$ -GO) hybrids can be added to epoxy to considerably improve its corrosion-resistant performance. As indicated in Figure 5, Yu et al. [41] observed the morphology of coatings during the corrosion process and highlighted the effect of  $\text{TiO}_2$ -GO. As revealed in Figure 5,  $\text{TiO}_2$ -GO hybrids clearly outperform conventional nanofillers, such as  $\text{TiO}_2$  and graphene oxide (GO), in terms of improving the corrosion resistance of epoxy coatings at the same contents. The exfoliation, dispersion, and good micro-pore plugging properties of the  $\text{TiO}_2$ -GO hybrids, which result from their laminated structure, contribute to their superiority.

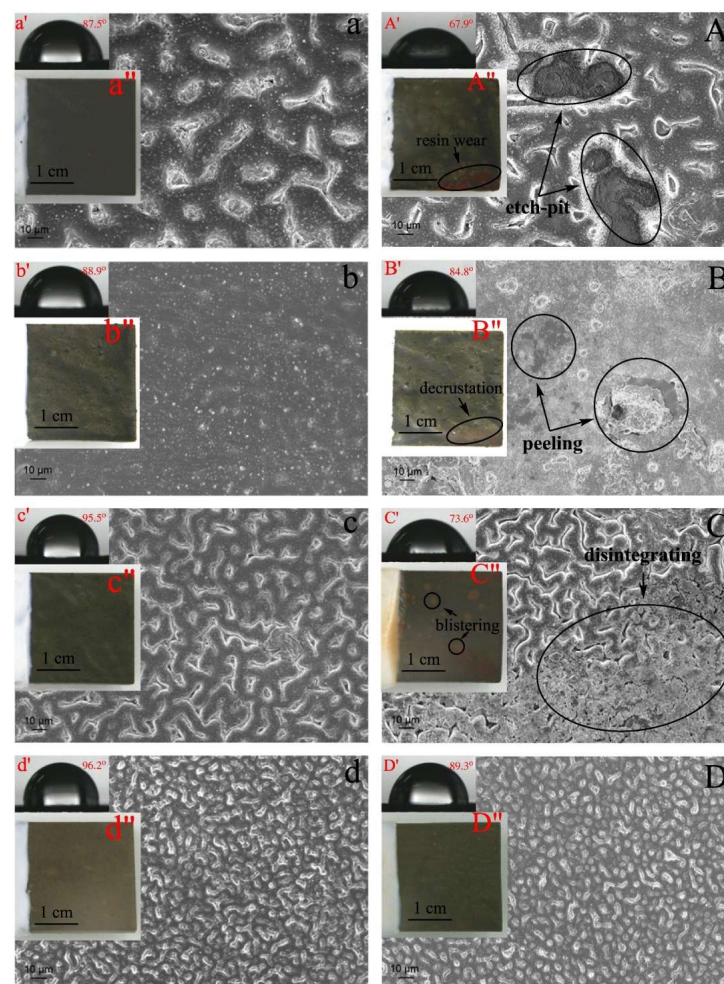


**Figure 5.** SEM images of coated steel samples; (a) pure epoxy, (b) 2 wt.% GO/epoxy, (c) 2 wt.% nano- $\text{TiO}_2$ /epoxy, and (d) 2 wt.%  $\text{TiO}_2$ -GO/epoxy before immersion, and their corresponding images after 20 days of immersion (A–D). Inset: water contact angle and surfaces of samples. Reproduced with permission [41], copyright 2015, Elsevier.

#### 2.4. Biopolymer Coatings

Biopolymers are obtained from biological and sustainable resources by biochemical conversions with or without catalysts [42]. Biopolymers are high-molecular-weight macromolecules. Examples are polysaccharides, polypeptides, and polynucleotides with repeating units linked by covalent linkages. The addition and removal of these repeating units do not alter the chemical characteristics of the polymer. They are classified based on the source of origin, linkages involved, physical, chemical, thermal characteristics, etc. [43]. Biopolymers can be plant-based, involving polysaccharides such as cellulose and starch. In addition, animal/insect/microbial biopolymers like chitin, collagen, lipids, polypeptides, and polylactic acid exist. These biopolymers are chosen due to their biocompatibility, reabsorption properties, and non-toxic nature. The molecular weight of the biopolymer is dependent on its viscosity and solubility.

Biopolymers such as cellulose are functionalized by replacing the hydroxyl group with ether, acetyl, or ester derivatives to form hydroxyl ethyl cellulose, hydroxyl ethyl methylcellulose, hydroxyl methyl propyl cellulose, and carboxyl methylcellulose. Biopolymers form films for developing water-borne coatings and can also be used as a thickening agent in paints and protective ingredients in emulsion paints. Blending gelatin with other biopolymers such as soy protein, polysaccharides, vegetable oil, etc., can enhance their coating performance [43]. Biopolymers used in the coatings are eco-friendly and sustainable. Using such biopolymers will reduce dependence on petroleum-derived polymers that are non-biodegradable and leave a carbon footprint. Biobased polymer coatings are preferred in developing biomaterials and films in various fields such as biomedical devices and anti-corrosive materials. The bio-coating performance of these biopolymers can be enhanced by blending the biomaterials with plasticizers and compatibilizers. Biopolymer-based coatings are hydrophilic and can be coated with antimicrobials to develop suitable biomedical materials for preventing pathogenic infections. Some natural polymers in biobased coatings possess antioxidant and antimicrobial activity (antibacterial/antifungal).

Dastpak et al. [44] used the Tafel method in a 3.5 wt.% NaCl solution to determine the corrosion performance of samples with and without oxide or lignin coatings. Figure 6 shows that the most corrosion-prone material is bare S355 steel. In contrast, when a plasticized lignin (PL) coating was applied to the surface, the corrosion current density reduced while showing a slightly higher corrosion potential. Compared to bare steel, steel samples with an anodized oxide layer but no coating (O-24, O-50, and O-128) all show a decreased corrosion rate. Still, they are not as effective as the lignin coating on the same substrate (Figure 6a). This is ascribed to the lignin's inert characteristics, which can block electrochemical processes at both the cathodic and anodic branches and further block the steel surface from the corrosive electrolyte. As revealed in Figure 6b, the corrosion current density for all three anodized surfaces (O-24 + PL, O-50 + PL, and O-120 + PL) is significantly reduced because of the application of lignin coatings.

As a shortcoming, some of the biopolymers used experience poor mechanical strength. To overcome this limitation, surface modifications using plasticizers and surfactants are added, improving their functionality for various applications. The high viscosity of biopolymers can interfere with the formation of uniform coatings on the surface. In some cases, high temperatures and harsh chemicals are required for extracting the biopolymers example, chitosan. In the long run, plasticizers may detach from the biopolymer coatings.



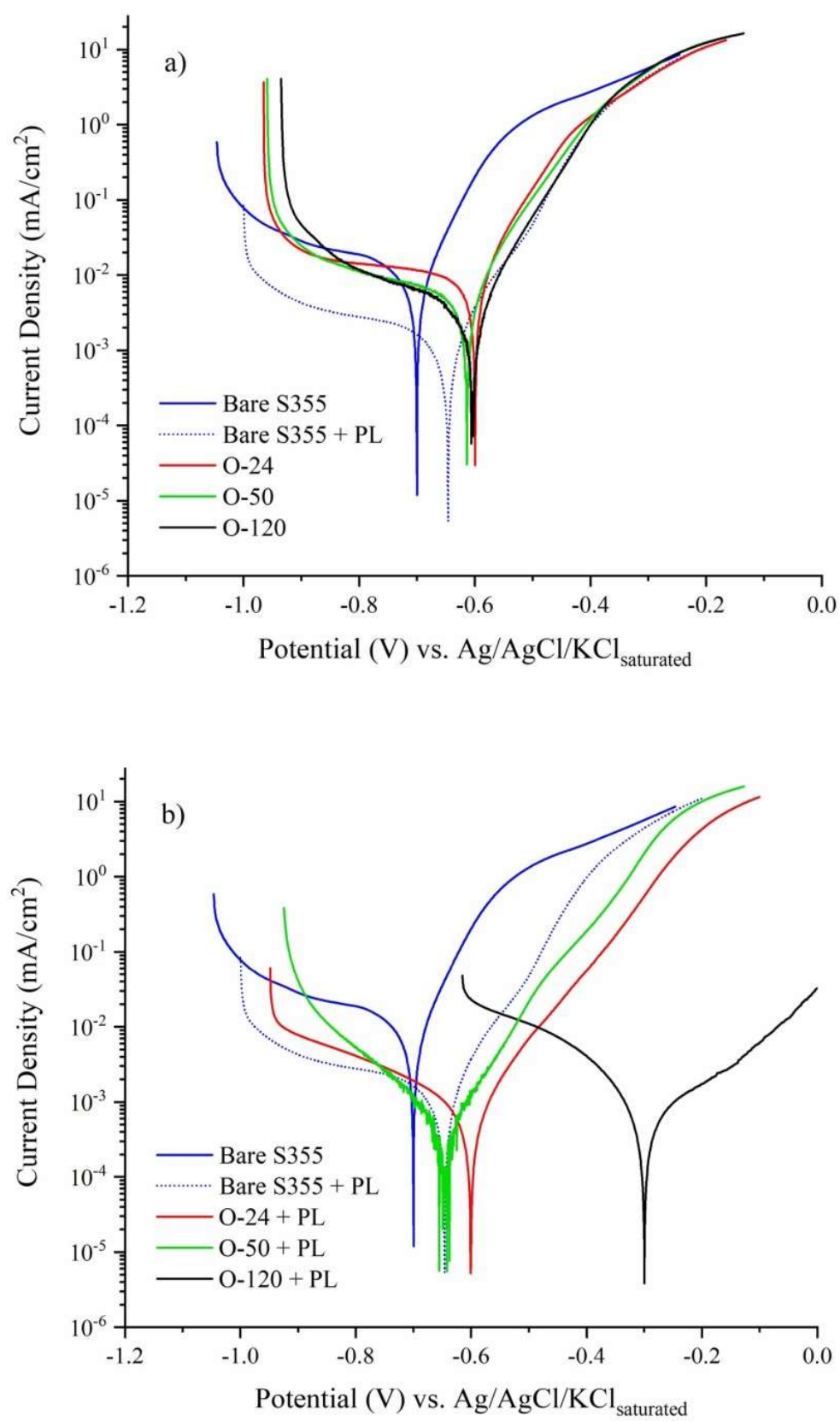


**Figure 6.** Tafel plots for the bare steel and anodized surfaces (a) before and (b) after adding plasticized lignin coatings. Reproduced with permission [44], copyright 2020, Elsevier.

### 2.5. Other Polymeric Coatings

Acrylic resin coatings are polymeric resin coatings with outstanding adhesion, weathering, and anti-corrosive properties alongside abrasion and chemical resistance [45]. Alkyd coatings are another class of polymeric resin coating advantageous for fabricating modifiable anti-corrosive coatings [46]. Alkyd coatings can be water-borne or otherwise. Furthermore, unsaturated polyesters, poly (ether imide), styrenics, and polyenes are non-polar hydrophobic polymers capable of protecting metals from corrosion triggers. Being non-polar, adding anchoring groups/compounds will improve their adhesion to the metal substrate [47].

### 3. Polymeric Coating Performance in Different Corrosive Environments

The exposure of iron and steel in the natural environment results in the formation of rust. Metals corrode, but non-metallic substrates also deteriorate on exposure and with time. The losses incurred due to corrosion are enormous and are a worldwide issue. Furthermore, different operational environments influence corrosion in diverse ways, as metallic surfaces differ in structure and composition. Since corrosion is an electrochemical process, the anode, cathode, and electrolyte form an electrical cell at the corrosion site [2].

Polymeric organic coatings are applied to metallic substrates to avoid corrosion's detrimental effect. These are permeable coatings, and for the non-superhydrophobic types, the defects are pathways for the penetration of corrosive species to the metal surface—resulting in localized corrosion. Pigments/additives with lamellar or plate-like shapes, such as mica-ceous iron oxide and aluminum flakes, have been introduced to polymeric coatings [48]; the presence of these flakes increases the diffusion paths' length for the destructive species. Similarly, graphene, carbon nanotubes, silica, and zirconia nanomaterials have also been utilized. A good barrier effect depends on the orientation and compatibility of the inclusions in the coating matrix. The parallel configuration of the inclusions in the coating matrix to the surface is ideal. Similarly, layered clay platelets such as montmorillonite loaded in organic resins also increase the barrier effect by preventing the penetration of oxygen and water molecules; thereby, enhancing the anti-corrosive performance of the coating [49]. Particles in the microscale have also been very beneficial.

The performance of polymeric coatings in corrosion prevention depends upon parameters such as the adhesion of the coating layer to the metal, the thickness of the coating, water, acid, base resistance, permeability, etc. The primer layer plays the dual role of protecting the metal closest to it and adhering to the other layers of the coating applied to it. Various anti-corrosive polymeric film analyses can be achieved by applying multiple effective tests. These tests reveal the changes during the film's interaction with the harsh environment and the effect on the underlying metal substrate. The thickness of the coating and the exposure duration play critical roles when determining the coating performance. Laboratory tests, such as electrochemical testing, water uptake, adhesion, immersion test, salt spray test, cabinet test, leaching test of detached film, etc., have been widely utilized to examine the efficiency of the coatings in diverse corrosive environments [50]. It should be noted that the inhibitor-loaded carriers' proximity to the metal/alloy surface should not be compromised. In addition, compatibility of the coating matrix with the inhibitor-loaded carriers, fillers, and blends should be ensured.

Different corrosive solutions/solvents have been used to investigate the corrosion protection of metals and alloys, whether coated or not. Examples of corrosive solutions investigated include artificial seawater (NaCl), acids (HCl & H<sub>2</sub>SO<sub>4</sub>), bases (NaOH, KOH), strong oxidizers (hydrogen peroxide, nitric acid, nitrate, and nitrite compounds, perchloric acid and perchlorate compounds, and hypochlorite compounds), Hank's solution (Hanks' Balanced Salt Solution (HBSS)), Harrison's solution (0.35 wt.% (NH<sub>4</sub>)<sub>2</sub>SO<sub>4</sub>), etc. Presented in Table 1 is a list of selected polymer coatings where highlights of the studies are summarized in different corrosive media where steel substrates were utilized.

**Table 1.** Selected polymeric coatings and their summarized performances in corrosive environments.

S/N	Polymer Matrix	Fillers/Blends/ Pigments	Metals/Alloys Coated	Corrosive Media	Coating Thickness	Immersion Time	Investigation Techniques	Findings/ Remarks
1.	Epoxy blend from bisphenol A diglycidyl ether (BADGE) and Neopentyl glycol diglycidyl ether (NGDE) epoxy monomers and curing agent; Jeffamine D230 [51]	Carnauba wax microparticles	Q235 carbon steel	3.5 wt.% sodium chloride (NaCl) solution	50 ± 5 µm	7 days	Electrochemical impedance spectroscopy (EIS), Scanning electrochemical microscopy (SECM)	At 65 °C, the shape memory effect can seal cracks in the coating. At 90 °C, melted carnauba wax caused a complete crack sealing.
2.	Polyurethane [21]	Polyurea microcapsules/linseed oil as the active healing agent	Steel panels	5% NaCl aqueous solution	-	120 h maximum	Accelerated corrosion test	A 2 to 5% increase in microcapsule contents decreased corrosion and blistering at the defects after 120 h of immersion.
3.	Polyurethane (PU) [22]	α-zirconium phosphate nanoplatelets	Cold-rolled steel (CRS) electrodes	3.5 wt.% NaCl aqueous solution	30–36 µm	-	EIS and Potentiodynamic polarization	ZrP-5/PU-coating showed a corrosion rate 35 times less than PU coating.
4.	Waterborne polyurethane [52]	3-aminopropyl-trimethoxysilane modified Cloisite 30B	Mild steel	3.5% NaCl solution	-	7–17 days	EIS and 5% salt spray assessment	Superior corrosion-inhibiting properties of CPU0.5 and CPU1 were observed due to the barrier effect provided by the clay nanoparticle-modified coatings.
5.	Alkyd primer [53]	Dodecylamine deposited on silica nanoparticles and encapsulated in polyelectrolyte shells	Carbon steel AISI 1020	0.01 mol/L NaCl	100 µm total dry thickness	48–96 h	EIS, Scanning vibration electrode technique (SVET), and salt spray tests.	10 wt.% of the nanocontainer-loaded coatings provided the best self-healing properties for the coating.
6.	Cardanol-based epoxy [54]	-	Mild steel	5 wt.% NaCl solution	50 µm and 150 µm	21–180 h	Salt spray humidity cabinet test	Solvent-free epoxy and hardener were produced from cardanol as a biobased anti-corrosive coating for steel without inhibiting fillers or pigments. The best film integrity was that of 2:1 wt.% cardanol-based epoxy and hardener after the anti-corrosion test, for which the highest adhesion strength, lowest permeability, and fewer blisters were obtained.
7.	Epoxy [55]	Amino propyl trimethoxy silane (APS) treated ZrO <sub>2</sub> nanoparticles	Mild steel	3.5% NaCl solution and 5% NaCl solution	45 ± 5 µm	EIS: 120 days, ECN: 7 days, and Salt spray: 2000 h,	EIS, electrochemical noise (ECN) techniques, and salt spray test	The treated nanoparticles interacted with the polymer matrix, which enhanced its barrier performance. 3 wt.% of the ZrO <sub>2</sub> nanoparticles provided the maximum resistance values.

Table 1. Cont.

S/N	Polymer Matrix	Fillers/Blends/ Pigments	Metals/Alloys Coated	Corrosive Media	Coating Thickness	Immersion Time	Investigation Techniques	Findings/ Remarks
8.	Epoxy ester [56]	<i>Cichorium intybus</i> L. leaf coupled with zinc acetate to give a hybrid pigment extract	Mild steel	3.5 wt.% NaCl	$60 \pm 5 \mu\text{m}$	24 h for EIS and 300 h for salt spray test	EIS and salt spray test	The hybrid pigment-based coating exhibited capacitive behavior throughout the studied frequency range with a high impedance value ( $ Z $ at 10 mHz) $> 10^{10} \Omega \cdot \text{cm}^2$ even after nine days of immersion.
9.	Acrylated polycaprolactone polyurethane [57]	2-Mercaptobenzothiazole (MBT) inhibitor loaded into layered double hydroxide (LDH)	Hot-dip galvanized steel (HDG)	0.05 M NaCl solution	100 $\mu\text{m}$	48 h	EIS and SVET	MBT was released in the coating defect, and the application of heat above 60 °C to the coated sample for 2 min sealed the defect, preventing a corrosion attack.
10.	Poly[(vinyl butyral)-co-(vinyl alcohol)-co-(vinyl acetate)] (PVB)-matrix [58]	pH-responsive poly(styrene-stat-methacrylic acid) (PSMAA) nanocapsules filled with Grubbs–Hoveyda second-generation catalyst and dicyclopentadiene (DCPD) healing agent	Steel	1 M Potassium chloride (KCl)	$20 \pm 10 \mu\text{m}$ for the PVB coating	937 min	scanning Kelvin probe (SKP) technique	The self-healing agent (norbornene derivative of DCPD) was attached to the zinc nanocomposite coating. PVB matrix was applied to this, and a bilayer self-healing coating was achieved with binding effects obtained from PVB.
11.	Alkyd varnish [59]	Hexamethylene diisocyanate (HDI) biuret microcapsules as additives	Q235 steel	0.6 M NaCl	200 $\mu\text{m}$	1500 h	EIS and alternating current mode of SECM (ACSECM)	The impedance values of the coating were observed to increase initially gradually. As time progressed, a decrease was observed as the healing agent became exhausted, and as water penetration occurred, corrosion products filled the crevice competing for healing.
12.	Chitosan [60]	-	Mild steel	0.5 M $\text{H}_2\text{SO}_4$ solution	-	48 h maximum	EIS and potentiodynamic polarization	The chitosan film was electrophoretically deposited on the steel samples. An inhibition efficiency of 98.1% in the acidic electrolyte was achieved.
13.	Epoxy resin [61]	Polyaniline (undoped, doped with HCl sulfonated (SPAN), and fibers), zinc phosphate pigment, zinc chromate pigment	Mild steel	3.5% NaCl solution	$110.9 \pm 2.7 \mu\text{m}$ – $180.2 \pm 4.8 \mu\text{m}$	24–1728 h	EIS	The passive film formed in the defects contained a mixture of oxides ( $\text{Fe}_2\text{O}_3$ and $\text{Cr}_2\text{O}_3$ ) from the interaction of the exposed metal surface and the leached pigments.



Table 1. Cont.

S/N	Polymer Matrix	Fillers/Blends/ Pigments	Metals/Alloys Coated	Corrosive Media	Coating Thickness	Immersion Time	Investigation Techniques	Findings/ Remarks
14.	Alkyd resin [62]	ZnO nanoparticles pigment. Benzotriazole inhibitor entrapped in between polyaniline and polyacrylic acid (PAA) polyelectrolytes	Mild steel	5% HCl, NaCl, and NaOH solutions	50 $\mu\text{m}$	168 h maximum	Potentiodynamic polarization	A positive shift of the $E_{\text{corr}}$ value was observed for 5 wt.% benzotriazole inhibitor entrapped nanocontainers-based alkyd coatings. Chemisorption of the released inhibitor from the affected alkyd coating formed a passive layer, a complex film that reduced the penetration of corrosion species.
15.	Epoxy-Polyamide [63]	poly (o-anisidine) (PoA) nanoparticles	Carbon steel	NaCl (5 wt.%) and HCl (5 wt.%)	110–135 $\mu\text{m}$	15 days in NaCl solution	EIS and potentiodynamic polarization	In a saline environment, the co-polymer nanocomposite coating showed enhanced protection due to the strong electrostatic interaction between the filler and the matrix, preventing corroding species' penetration. In the acid environment, the presence of the phenazine skeleton in the ladder polymer provided the blocking effect for transporting corroding species to the metal-coating interface.
16.	Epoxy vinyl ester and epoxy-amine [64]	Polydimethylsiloxane (PDMS) as healing-agent-filled in urea-formaldehyde microcapsules and dimethyldineodecanoate tin (DMDNT) catalyst-filled polyurethane microcapsules	Cold-rolled steel	5 wt.% aqueous NaCl solution and 1 M NaCl solution	100–150 $\mu\text{m}$	120 h	Immersion and electrochemical test	All control samples corroded within 24 h within the scribed region, while self-healing coatings showed no evidence of rust even after 120 h exposure to the electrolyte. A combination of the healing agent and the catalyst influenced self-healing. The adhesion promoter showed no interference.
17.	Alkyd primer [65]	Entrapped-dodecylamine in Halloysite nanotubes (HNTs)	Carbon steel	0.01 mol/L NaCl	~200 $\mu\text{m}$	8 h maximum for EIS, 12 h for SVET, and 720 h maximum for salt spray test	EIS, SVET and salt spray test	10 wt.% of HNTs loaded dodecylamine provided self-healing triggered by pH changes in the defect area of the coating, inhibiting the kinetics of the corrosion process.

Table 1. Cont.

S/N	Polymer Matrix	Fillers/Blends/ Pigments	Metals/Alloys Coated	Corrosive Media	Coating Thickness	Immersion Time	Investigation Techniques	Findings/ Remarks
18.	Water-borne Alkyd [46]	Benzotriazole-loaded mesoporous silica nanoparticles (MSN) in the presence of tannic complexes	Mild steel	0.1 M NaCl	-	20 days	EIS and potentiodynamic polarization	2 wt.% of Inhibitor-loaded MSN provided a significant self-healing effect after 20 days of immersion in the corroding medium. The tannic complex (coordination complex of tannic acid (TA) and Fe <sup>3+</sup> ion) provided a non-spontaneous pH release action for the entrapped corrosion inhibitors.
19.	Polyurethane (PU) from algae oil [66]	-	Mild steel	3.5 wt.% NaCl and 0.5 M HCl solutions	120 µm	7 days	Potentiodynamic polarization	An outstanding result was attributed to the PU coating containing sulfur bonds. Coatings evaluated in the salt solution performed better than those assessed in the acid medium due to the polar ester group breaking by hydrolysis in HCl. Furthermore, the mercaptosuccinic (MSA) and thiodipropionic (TPA) PU-based coatings showed satisfactory antimicrobial effects against <i>E. coli</i> and <i>S. aureus</i> .
20.	Hyperbranched Soya Alkyd (HBA) and HBA-Butylated melamine-formaldehyde (BMF) [67]	Magnetite nanoparticles as fillers	Carbon steel	3.5 wt.% NaCl	-	7 days	EIS, Potentiodynamic polarization, and salt mist test	The magnetite nanoparticles improved the nanocomposite coating's impact resistance and scratch hardness.
21.	Acrylated polycaprolactone Polyurethanes [68]	-	Hot-dip galvanized (HDG) steel	0.05 M NaCl solution	100 µm	13 days maximum	EIS and SVET	The impedance modulus of the coating after healing is almost the same value before the coatings were scratched. In the absence of corrosion inhibitors and other corrosion-inhibiting fillers, the polymer coatings showed adequate metal protection due to the shape-recovery properties of the polymers.
22.	Acrylonitrile-butadiene-styrene (ABS) [69]	Outdated lansoprazole medicine as a corrosion inhibitor	Commercial 1018 steel	3% NaCl solution	-	2000 h	EIS, potentiodynamic polarization, and electrochemical noise (ENM)	Lansoprazole, one of the gastric secretion suppressors, served as an effective organic corrosion inhibitor blended in ABS. Coating efficiency as a function of time was above 80% throughout.

#### 4. Metal–Organic Frameworks (MOFs) as Functional Additives in Polymer Coatings

The reaction between metal cations and organic ligands produces metal–organic frameworks (MOFs), commonly known as porous polymers/coordination polymers. MOFs have emerged as a viable contender with several unique and adaptable features, including large surface area, porosity, a wide range of compositions, a versatile and customizable pore structure, high crystallinity, and tunable functionality. MOFs' structural, physical, and chemical properties can be altered by modifying the size, shape, and length of linkers, composition, three-dimensional configurations, and pre-and post-synthetic modification. As a result, they are suitable for research in various domains and applications [70]. Researchers have paid close attention to three-dimensional (3D) nanostructure MOFs, one of the subdivisions of sophisticated coordination polymers, because of their unique features. MOFs have a high interior surface area, and about 90% of their internal volume is open space, making them suitable host molecules. The production of diverse MOFs is caused by the coordination of metal cations/oxide groups with polyatomic hetero-atom-bearing organic ligands via the donor–acceptor mechanism [71].

The versatility of MOFs has attracted enormous attention leading to their use for catalysis, drug delivery vehicles, gas storage or separation, and biological imaging. MOFs have been used to create materials for supercapacitors, fuel cells, rechargeable batteries, electrocatalysis, and corrosion prevention in electrochemistry [72]. MOFs are good candidates for catalysis, highly efficient adsorbents for selective separation, and storage for gases like H<sub>2</sub> and CH<sub>4</sub> because of their loading and releasing properties. Wound healing, anticancer, antimicrobial, and medication loading are only some of the biomedical applications. MOFs have become popular due to their benign and bioactive properties [71].

The structure of MOFs is sustained by weak cooperative interactions such as H-bonding, p–p stacking, and van der Waals interaction, in addition to the donor–acceptor interaction in coordination bonding. Because of these minimal forces of attraction, structural flexibility can be achieved even in relatively moderate conditions [72].

##### 4.1. Design and Synthesis of Metal–Organic Frameworks (MOFs)

MOFs have some advantages over other organic corrosion inhibitors, including the ability to be synthesized with affordable precursors and high-yield synthesis methods at low temperatures (25 °C). Metal–ion precursors are usually cheap, such as inorganic salts such as nitrates, sulphates, and chlorides. Multidentate ligands like carboxylate, azoles, and nitriles are common organic ligands. The linkage molecules frequently intend to redirect the incoming/repeating ligand units in a specific direction without affecting the end product's formula [72].

Solvent evaporation and isothermal synthesis, hydro(solvo) thermal synthesis, ultrasonic- and microwave (MW)-assisted pathways, diffusion method, mechanochemical method, and electrochemical (EC) synthesis are the major techniques employed in the production of MOF skeletons. Each has its own set of benefits and drawbacks. The most used methods and the conditions used in the experiments [71] are depicted in Figure 7.

##### 4.2. Anti-Corrosion Potential of Metal–Organic Frameworks

MOFs can be incorporated into corrosion protection action in different ways. They may act as carrier molecules for incorporating potential inhibitors (organic/inorganic) in corrosive medium or pickling solutions; they can be added as potential corrosion inhibitors. The MOFs alone or when loaded with other potent inhibitors can be dispersed in polymer systems like epoxy or polyurethane coatings to enhance the potential of polymer coatings or can be included as a part of composite coatings for corrosion inhibition.

##### 4.2.1. Metal–Organic Frameworks (MOFs) as Containers for Loading Inhibitors

MOFs alone or combined with other materials can be used as containers for loading corrosion inhibitors. Zhao et al. prepared GO/MOFs nanocontainers by in situ growing two different MOFs on the graphene oxide (GO) sheets and encapsulated benzotriazole molecule

to produce GO/ZIF-8@BTA or GO/UiO-66@BTA-loaded nanocontainers (Figure 8I). The coating containing this nanocomposite exhibited good corrosion inhibition by passive and active protection; although, this was achieved with a copper substrate and not mild steel. However, the idea via one-pot reaction can be extended to other MOFs to load different inhibitors to protect different metals. Where the barrier protection property of GO ensures passive protection, the highly porous nature of MOFs results in good adsorption capacity. At the same time, the inhibitors released from the MOFs on pH stimulation are responsible for active protection [73].

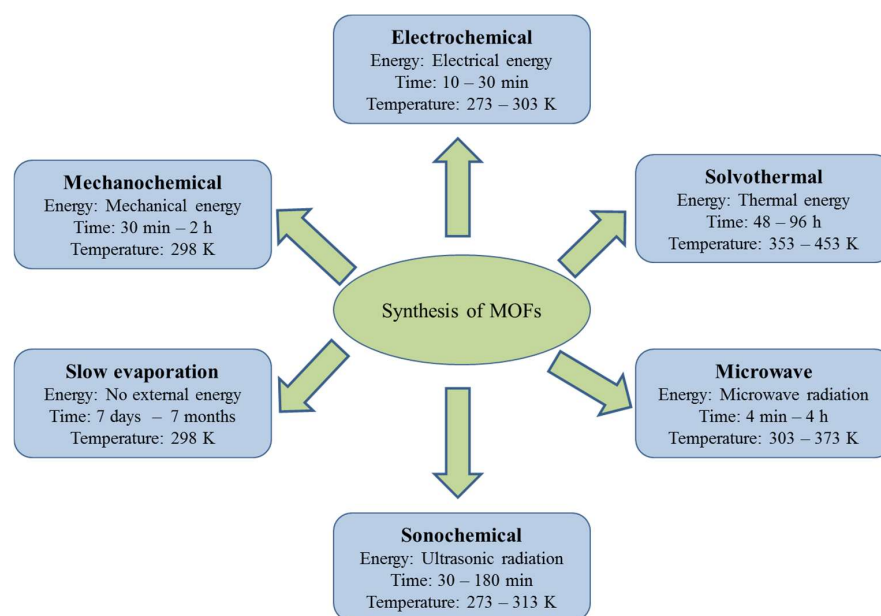


**Figure 7.** Various methods for the preparation of the MOF compound. Reproduced and adapted with permission [71], copyright 2021, Elsevier.

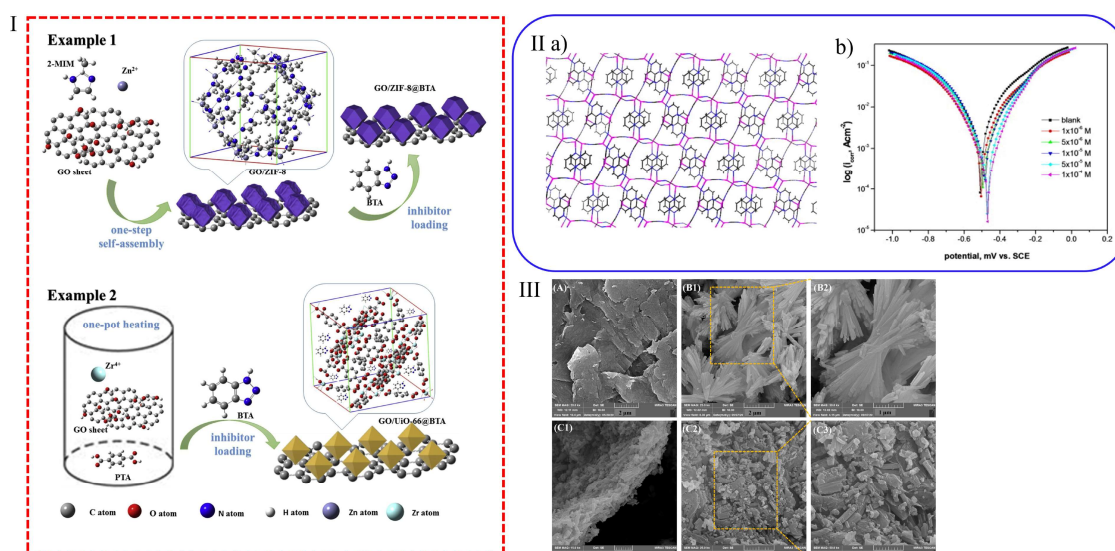


**Figure 8.** (I) Synthesis approach of loaded GO/MOFs nano-containers. Reproduced with permission [73], copyright 2020, Elsevier. (II) (a) 3D-network arrangement of interwoven [(AgCN)<sub>4</sub> (qox)<sub>2</sub>] along the a-axis. (b) Tafel plot for corrosion analysis of C-steel with different inhibitor concentrations. Reproduced with permission [74], copyright 2011, Elsevier. (III) FE-SEM images of (A) GO nanosheets (B1,B2) Ce-MOF NPs with different magnifications, (C1–C3) GO@Ce-MOF NPs from different angles and various magnifications. Reproduced with permission [75], copyright 2021, Elsevier.



In another study, Tian et al. used MOFs for the controlled delivery of a triazole derivative with many active groups for the corrosion inhibition of MS in 0.5 M sodium chloride solution. In the potentiodynamic polarization studies, 98% inhibition efficiency was observed by suppressing both anodic and cathodic reactions by forming a protective layer. The controlled delivery of inhibitor from the container, which allows for a longer film growth time on the steel surface, significantly improved inhibition by causing the insoluble protective layer to densify. Furthermore, it was reported that the used MOFs could be effectively recycled at least five times with a minor reduction in loading ability [76]. Moreover, considering the properties of selected active substances intercalated in MOFs can lead to further improvements in their performance. For example, Li et al. loaded the Cetyltrimethylammonium bromide (CTAB) molecule in HKUST-1(MOFs) to prepare CTAB@HKUST-1. CTAB was selected because it contains both hydrophilic and hydrophobic ends and proved to selectively locate in the pores of the HKUST-1 coating on a metallic surface. A thin film of this inhibitor was successfully coated on the metal surface by an electrophoretic method. The CTAB@HKUST-1 films exhibited excellent corrosion inhibition potential. The inhibitor loading in MOFs showed active corrosion inhibition inside the defects and improved the overall coating stability of CTAB on the metal. The stability of the MOFs will decide the activity of the coating [77].

#### 4.2.2. Metal–Organic Frameworks (MOFs) as Corrosion Inhibitors

The use of MOFs as corrosion inhibitors has also received attention. The corrosion inhibition properties of a molecule rest on its physicochemical properties such as structure, size, active chemical groups, aromaticity, electron donating ability, etc. In many cases with metals, organic moieties containing heteroatoms such as N, P, O, or S are excellent inhibitors. Like coordination compounds, MOFs with different ligands combined with metal ions are also excellent corrosion inhibitors as most contain heteroatoms with lone pairs of electrons or pi electron cloud [72]. For instance, Etaiw et al. synthesized brown crystals of  $[(\text{AgCN})_4(\text{qox})_2]$ , created by the interaction of  $\text{AgNO}_3$ , quinoxaline (qox), and KCN [74]. The inhibitor role of the MOF in 1N HCl for carbon steel was studied.  $[(\text{AgCN})_4(\text{qox})_2]$  was chosen because of the presence of pi-electron systems that are stacked in parallel via H-bonds and  $\pi$ - $\pi$  stacking (Figure 8(IIa)) and the presence of heteroatoms which enables strong adsorption on the metal surface. The inhibition efficiency of the MOFs on steel was tested in 1 N HCl solution. The  $E_{\text{corr}}$  and  $i_{\text{corr}}$  values were analyzed at various amounts of the inhibitor varying between 0 to  $10^{-4}$  M in 1 N HCl. This resulted in the suppression of both branches of the polarisation curve, but the suppression was more prominent in the anodic branch (Figure 8(IIb)). In the Tafel plot, both curves changed in parallel with increasing concentration of MOF, which indicates the blocking action of the MOF and adsorption on the metal (Langmuir adsorption isotherm). From the EIS studies, the charge transfer resistance was found to be increasing with increasing concentration of the inhibitor MOFs. The adsorption of the inhibitor to the metal surface was proposed to occur via a non-bonding interaction of lone pairs on nitrogen atoms with metal atoms, indicating a parallel arrangement of the aromatic rings with the metal surface. The authors further prepared yellow crystals of the MOFs  $[\text{Ag}(\text{qox})(4\text{-ab})]$  synthesized from  $\text{AgNO}_3$ , quinoxaline (qox), and 4-aminobenzoic acid (4-aba) [78]. Non-covalent interactions resulted in a three-dimensional network morphology. The corrosion inhibition potential of prepared MOFs was tested for steel in 1 N HCl solution using EIS and potentiodynamic polarisation analysis. Because of the abundance of electron-donating groups and pi systems, it exhibited an excellent corrosion protection rate (84% efficiency). The MOFs followed the Freundlich adsorption isotherm. In addition to lone pair and pi-electron donation, the complexes formed between the inhibitor cation and metal ions may adsorb onto the steel by Van der Waals forces to form a protective coating; thereby, preventing metal oxidation. The film protects the anodic and cathodic reactive sites and inhibits both reactions. Hence, it behaved as a mixed-type inhibitor.

For the first time, Keshmiri et al. fabricated an active/passive coating system using an eco-friendly, cerium-based MOF on GO nanosheets in an aqueous solution. The organic linker in the Ce-MOF nanoparticles was 1,3,5-benzene tricarboxylic acid, which resulted in a compact and straw-sheaf-like shape. The GO@Ce-MOF nanoparticles were then loaded into the polymer coating. Various techniques, such as SEM (Figure 8III), Raman spectroscopy, and TEM, were used to evaluate the successful production of nanoparticles. The EIS approach and a salt spray analysis were used to analyze the corrosion inhibition effectiveness of the produced nanostructures in the polymer matrix. Compared to the Blank/EP coating, the EIS data from the scratched surface after 48 h revealed a 500% improvement in GO@Ce-MOF/EP corrosion resistance. Furthermore, after seven weeks of immersion in corrosive solutions, the GO@Ce-MOF/EP coating demonstrated outstanding barrier qualities with low-frequency values greater than  $1010 \Omega \text{ cm}^2$ . Ce-MOF nanoparticles boost GO dispersion and the nanocomposite's potential active protective ability [75]. Therefore, the potential of MOFs has encouraged their application in several polymer coatings.

#### 4.2.3. Metal–Organic Frameworks (MOFs) in Polymer Coatings

In polymer coatings for anti-corrosive applications, MOFs have shown promise as a class of materials. The type of metal and ligand utilized, the synthesis procedure, and the formulation of the anti-corrosive coating all affect how well MOFs operate in them. Some of the major elements that can impact how well MOFs function in anti-corrosive coatings include:

1. Chemical stability: The effectiveness of MOFs as anti-corrosive coatings depends on their capacity to preserve structural integrity in corrosive environments, where they can be vulnerable to degradation.
2. Adhesion to the substrate: To effectively defend against corrosion, MOFs must attach firmly to the substrate surface. The coating composition, surface finishing, and substrate type might affect adhesion.
3. Barrier capabilities: MOFs can operate as a barrier to stop corrosive substances from penetrating the surface of the substrate. The porosity, crystallinity, and thickness of MOFs and other variables affect their barrier properties.
4. Self-healing capabilities: MOFs can have self-healing capabilities, which enable them to fix damages that develop to the coating over time. This could lengthen the coating's lifespan and boost its effectiveness.

Although organic coatings are considered the most effective, scratches and other defects interfere with their protective performance and allow for corrosion initiation. During the curing and drying process, micro-cracks and pores may form in the polymer interior, allowing corrosive ions from the environment to penetrate. A new area of dynamic coatings containing inorganic micro- and nano-containers loaded with organic polymers, corrosion inhibitors, polyelectrolytes, etc., has been developed [71]. Moreover, many attempts have been made to enhance polymer coatings' corrosion inhibition, toughness, and mechanical strength. The addition of fillers into the polymer was the major aspect tried. Compatibility between the organic and inorganic parts was the major issue to be addressed, which can result in agglomeration and defects in the matrix. Several nano/microparticles have been introduced to improve organic polymers' physical, mechanical, thermal, and corrosion inhibition nature. Incorporating micro/nano-MOFs into organic films is an exciting and feasible method to improve the thermomechanical characteristics of the coating. Compared with other nanofillers such as carbon black, alumina, and silica, MOFs are more compatible with organic polymers since the organic struts can interact very well with the polymeric matrix. These structures have also been reported to effectively dissipate the applied stress energies on the surfaces [79,80].

Therefore, the ability of MOFs to improve the mechanical properties of polymer coatings is one of its key advantages. For example, an excellent epoxy composite matrix with good anti-corrosion and thermo-mechanical capabilities was fabricated using a novel MOF-like nano-pigment. A one-pot, co-precipitation technique using covalent and/or

coordinate networking of cerium (III) ions and 2-methylimidazole as an organic linker in methanol solvent was employed to develop a nanoceria-decorated cerium (III)-imidazole network (NC/CIN) as a novel metal–organic network. DMTA, Tensile, EIS, and salt spray evaluations were used to assess the thermo-mechanical and anti-corrosion properties of the NC/CIN-included epoxy composite. From the investigation, the NC/CIN-contained epoxy composite showed exceptional barrier-inhibitive protection for MS in corrosive environments [81]. It is interesting to note that the high surface area and mechanical stability of MOFs inspire enhancement of the tensile strength, hardness, and scratch resistance of coatings. Therefore, the filler content of the coating and, thus, its mechanical properties, can be increased by using MOFs as filler materials. Moreover, using MOFs in polymer coatings also has the advantage of giving the coating more functionalities. MOFs can be fabricated with specific functionalities, including catalytic or sensing capabilities, and can be included in the coating. This makes it possible to produce coatings that actively participate in reactions or can sense and react to environmental changes.

Several works have explored the improvement of polymer coatings by incorporating MOFs. Tang and Tanase examined synthetic methodologies for the manufacture of MOFs and their composites and evaluated the corrosion inhibition potential of MOFs using different approaches. They discovered that MOFs incorporated in polymer matrices improved mixing efficiency and permeability compared to pure polymer membranes [82]. The addition of MOFs has benefits like self-healing property, prevention of leaching of inhibitors, effective delivery of active molecules to the reaction sites, the sustainable and on-demand release of the active molecules, and remaining as a sustained passive coating. Usually, there will be an interaction between the polar tail of the organic coating and the inhibitor, but incorporating the inhibitor in inert nano reservoirs can prevent these unwanted interactions and increase the structural integrity of the coating [83]. Furthermore, for better performance of a functional coating, it is necessary to enhance the fillers' compatibility and the polymer matrix's crosslinking density. Consequently, graphene oxide modified by zeolitic imidazolate framework-8 (ZIF-8) exhibits good compatibility in the epoxy medium. Moreover, because of its pH-dependent response property, ZIF-8 is extensively used for drug delivery [84]. This property can be helpful in protective coatings as a trigger for the controlled release of inhibitors. Thus, many studies focused on ZIF-8 nanocontainers took place. Li et al. successfully incorporated 2-Mercaptobenzimidazole (M) into ZIF-8 on GO nanosheets, which were subsequently embedded in epoxy coating to create a pH-sensitive and self-healing composite coating. Because M-ZIF-8/GO could react with polymer, the anti-corrosion performance of matrix coating was considerably improved, as were the compatibility of M-ZIF-8/GO and the crosslinking density of the epoxy coating. TEM and SEM micrographs and EDs image are given in Figure 9I, and schematics of the fabrication is shown in Figure 9(IIa), with FT-IR, UV-vis, Raman, XRD, XPS, and TGA characterizations shown in Figure 9(IIb–g), respectively. It is interesting to note that the filler content was 0.15 wt.%, and the thickness of the coatings was  $40 \pm 5 \mu\text{m}$  [85]. Therefore, with further optimization, better protection could be achieved.

Similarly, Ramezanzadeh et al. incorporated GO@ZIF-8 particles in epoxy coatings, and via the artificial scratch test, 70% enhancement in corrosion prevention was found after 72 h immersion compared to pure coating [86]. Therefore, GO@ZIF-8-based coatings have been demonstrated to be effective in the protection of steel. Moreover, Baohui Ren et al. demonstrated an environmentally friendly metallic corrosion inhibition by incorporating zinc gluconate in ZIF-8. EIS and potentiodynamic polarization studies (Figure 10I) exhibited excellent corrosion inhibition potential of the prepared ZnG@ZIF-8/EP coatings. Compared to ZIF-8/EP coatings, ZnG@ZIF-8/EP coatings have excellent long-term and accelerated corrosion resistance. The performance of ZnG+ZIF-8/EP was far better than EP, ZIF-8/EP, and ZnG+ZIF-8/EP coatings due to the uniform dispersion, reduction in porosity and defects, and controlled release [87]. Evidence abounds regarding using ZIF-8-based MOFs in polymer coatings [88,89].

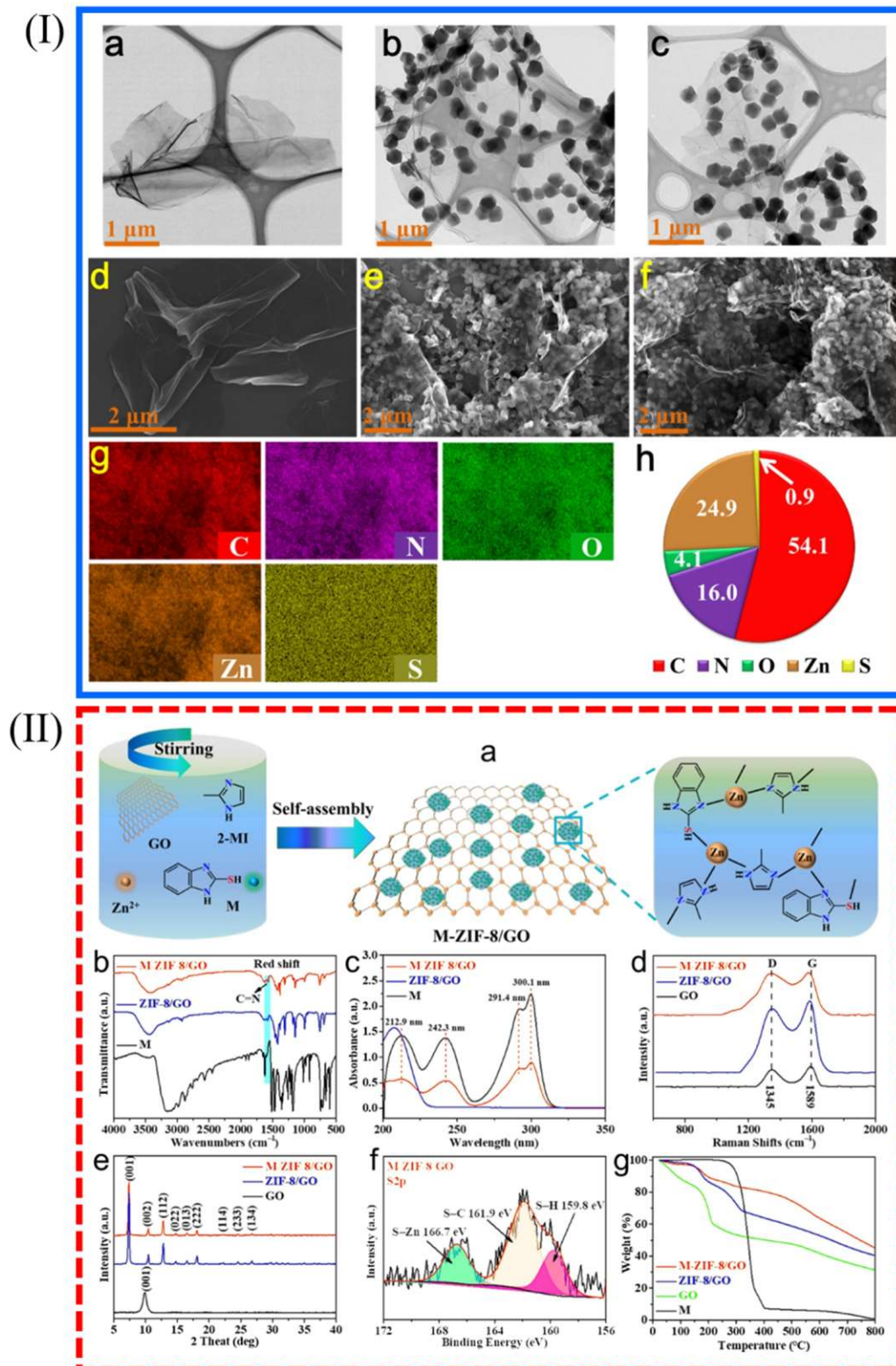


**Figure 9.** (I) TEM and SEM images of (a,d) GO, (b,e) ZIF-8/GO, and (c), (f) M-ZIF-8/GO, (g) SEM-EDS elemental analysis and (h) corresponding compositions of M-ZIF-8/GO (II) (a) Design of synthesis of M-ZIF-8/GO composite nanomaterial; (b) FT-IR and (c) UV-vis spectra (d) Raman and (e) XRD spectra (f) S2p high-resolution XPS spectra of M-ZIF-8/GO; (g) TGA curves. Reproduced with permission [85], copyright 2021, Elsevier.



Researchers have utilized many other MOFs in polymer coatings to achieve corrosion protection. In a study, Wang et al. grafted dopamine (DA) on the surface of MOF-5 to produce DA-MOFs which were embedded into waterborne epoxy coatings. Coatings with DA-MOFs exhibited excellent corrosion inhibition and hydrophobicity compared with pure epoxy coatings [90]. DA-MOFs' reaction with waterborne epoxy is given in Figure 10II. In another work on a graphene oxide (GO) substrate, Lashgari et al. constructed a ZIF-67 framework to obtain a new MOF subfamily.  $\text{Co}^{2+}$  and 2-methylimidazole were combined to make ZIF-67/GO NPs, which can be used to make epoxy-based corrosion-resistant coatings that are both active (self-healing) and passive. 3-Aminopropyl triethoxysilane (APS) was added to the ZIF-67/GO nanoparticles to improve particle compatibility with the epoxy medium and control their dissolution in saline solutions. The ZIF-67/GO@APS NPs were found to protect the steel surface by mixed-type inhibition and further demonstrated remarkable self-healing anti-corrosion performance [91]. Furthermore, Guo et al. developed a pH-triggered self-healing anti-corrosion coating based on benzotriazole incorporated in ZIF-7. Self-healing coatings demand a quick release of the inhibitors before the protective layer is damaged but must avoid unwanted leakage. Here, the authors utilized a ligand exchange approach to synthesize ZIF-7@BTA nanoparticles with 30 wt.% benzotriazole inhibitors. The as-synthesized ZIF-7@BTA on a scratch test exhibited 99.4% inhibition performance in acidic conditions by rapidly releasing the BTA inhibitor onto scratched areas (mechanism given in Figure 10III). Only less than 4% of the inhibitor leached out in a neutral medium [92]. In another work, zirconium-based nanoporous MOF (Glycidyl Methacrylate covalently functionalized Zr-UIO-66 MOF, Zr-UIO- $\text{NH}_2$ -MOF, and Zr- $\text{NH}_2$ -UIO-MOF particles were used as novel functional anti-corrosive additives) were incorporated in epoxy coating resulting in active and passive corrosion inhibition property of the improved coating [93].

Hybrid inhibitor systems can be achieved in polymer coatings with MOFs. An example is illustrated in work done by Nariman Alipanah et al. [94]. Organic-inorganic hybrid- $\text{Fe}^{3+}$ -based MOFs synthesized by hydrothermal reaction showed corrosion inhibition efficiency. The authors used the MOF MIL-88A (Fe) containing ferric ions and fumaric acid as a corrosion inhibitor. The presence of MIL-88A (Fe) in 3.5% saline solution showed a reduction in corrosion current, as shown by the potentiodynamic polarization curves in Figure 11. MILs belong to a class of metal-organic frameworks called Materials of Institute Lavoisier. MIL-88A (Fe) consists of nanoporous metalcarboxylates where fumarate is present with Fe. The inhibitor showed both active and passive protection in the corrosive medium. The released ferric ions and fumarate ions reacted with hydroxyl ions at the cathode, and the formed precipitate layer was deposited at the anode by sharing one pair of electrons of the oxygen atom. The formation of a protective coating was evident from the electrochemical studies (EIS) conducted in the saline extract of the metal-organic framework. As evident in Figure 12, the EIS test of the modified epoxy coating containing the FE-based MOF on a scratch test showed its ability for active corrosion inhibition. The Nyquist diagram (Figure 12) for the scratched epoxy coating containing the MOF showed more active corrosion protection for modified coating than the pure epoxy-coated sample.

Table 2 summarizes the recent application of MOFs in polymer-based anti-corrosion coatings.

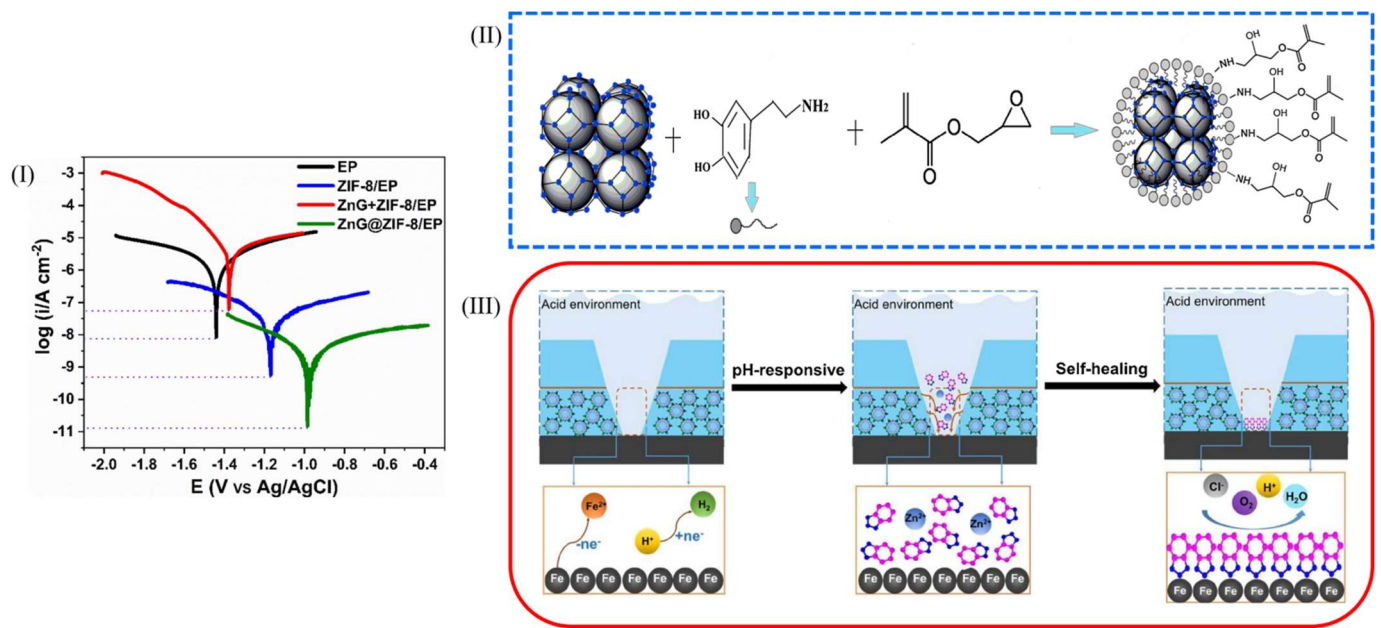


**Figure 10.** (I) Tafel plots of pure EP, ZIF-8/EP, ZnG+ZIF-8/EP, and ZnG@ZIF-8/EP coatings saline solution. Reproduced with permission [87], copyright 2020, Elsevier. (II) DA-MOFs reaction with waterborne epoxy. Reproduced with permission, copyright 2017, Elsevier. (III) Schematic representation for the self-healing action of the ZIF-7@BTA nanoparticles. Reproduced with permission [92], copyright 2019, Elsevier.

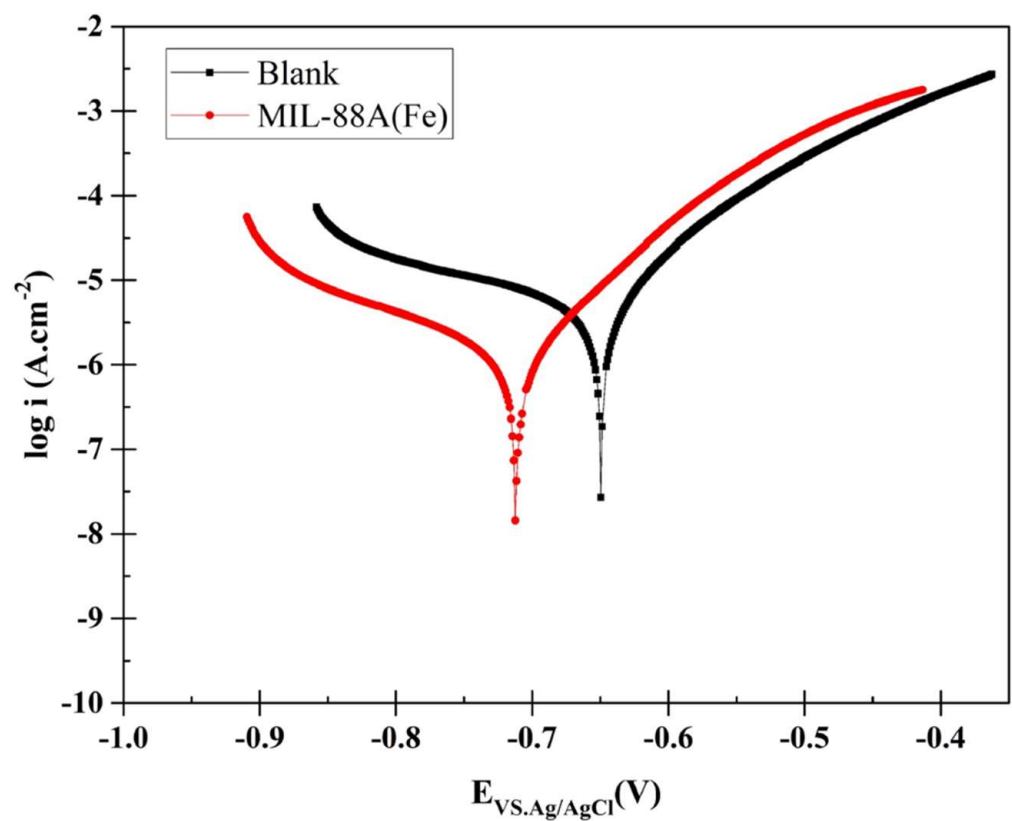


**Figure 11.** Tafel plot for bare steel substrates in the 3.5% saline solution after 3 h immersion in the presence and absence of the inhibitor MIL-88A (Fe). Reproduced with permission [94], copyright 2022, Elsevier.

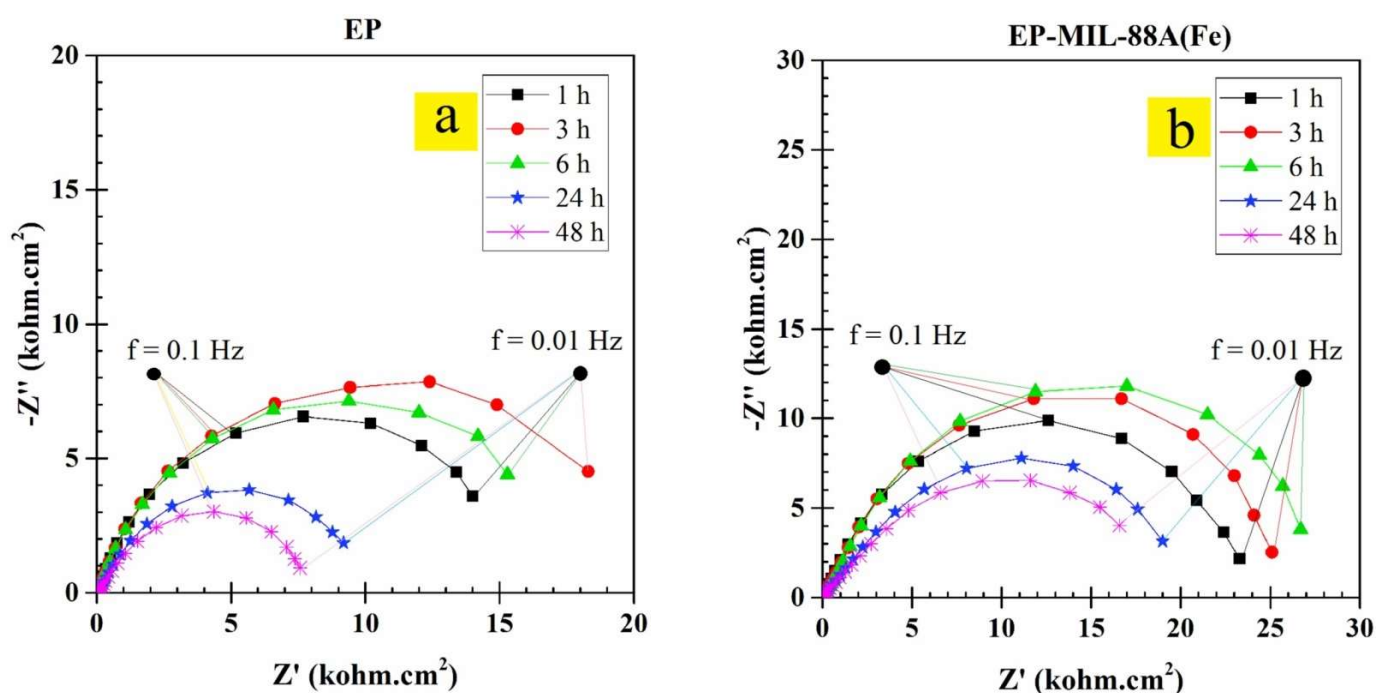


**Figure 12.** Nyquist plot for the (a) pure and (b) modified epoxy coatings in the scratch test experiment in 3.5% saline solution. Reproduced with permission [94] Copyright 2022, Elsevier.

#### 4.2.4. Protection Mechanism of MOFs

There are many factors affecting the corrosion inhibition mechanism of MOFs. It includes features such as ligands with heteroatoms containing a lone pair of electrons, aromatic systems with pi electron clouds, a structure and steric factor of the ligands, their arrangements in the space, and an ability to form a conjugate acid-base pair, hydrophobic nature, etc. Adsorption on the metal surface is the initial step in the inhibitory process in acid media. The creation of a donor–acceptor surface complex between the inhibitor’s  $\pi$ -electrons or lone pair of electrons and the metal’s unoccupied d-orbitals is proposed in most inhibition experiments.

Etaiw et al. describe the mechanism based on the inhibition action of MOF- [Ag(qox)(4-ab)] as follows. The inhibitor contains many nitrogen and oxygen atoms and an aromatic system. In the acidic medium, the inhibitor either remains neutral or has a cation (protonated form). Two types of adsorption mechanisms are possible for the replacement of water in this case: (1) the electrons in the heteroatoms or the pi electrons can interact with the d-orbital of the metal atom and can make a strong interaction by electron donation; (2) in an acidic medium the steel surface is positively charged so if the inhibitor exists as a cation, the direct interaction is difficult. The presence of a negatively charged  $\text{Cl}^-$  ion helps in adsorption by a synergic mechanism. In addition to electron transfer from inhibitor, another mechanism of metal–inhibitor complex formation also happens with freshly generated  $\text{Fe}^{2+}$  ions [78].

**Table 2.** Summary of MOFs as functional additives in polymer-based anti-corrosion coating.

S/N	Polymer Matrix	Fillers/Blends/Pigments	Metals/Alloys Coated	Corrosive Media	Coating Thickness	Immersion Time	Investigation Techniques	Findings/Remarks
1.	Epoxy [95]	MOF nanoparticle of UiO-66-NH <sub>2</sub> integrated with carbon nanotubes (CNTs) (UiO-66-NH <sub>2</sub> /CNTs)	Mild steel	3.5% NaCl solution		45 days	EIS, salt spray, contact angle measurement	Lower coating hydrophilic nature (leading to lower water uptake) and better additives uniformity resulted in better barrier performance of the coating.
2.	Epoxy [96]	UIO-66 nanoparticles	Steel		70 µm	500 h	Accelerated UV-A aging test, micro-hardness, surface roughness, contact angle	The presence of 1.2 wt.% UIO particles significantly improved the epoxy film's UV-shielding characteristics.
3.	Epoxy [85]	ZIF-8, 2-Mercaptobenzimidazole, graphene oxide nanosheets	Q235 steel	3.5 wt.% NaCl solution	40 ± 5 µm	60 days	EIS, salt spray	The “labyrinth effect” and physical barrier effect may be present in GO nanosheets. The M-ZIF-8/GO/EP coating's high adhesion force, tensile strength values, and lowest water absorption rate demonstrated strong crosslinking density, few defects, and noticeable interfacial interaction with the metal substrate.
4.	Epoxy [97]	Nanoporous cobalt-based ZIF-67 MOF	Mild steel	3.5 wt.% NaCl solution	50 ± 5 µm	50 days	EIS, salt spray, pull off test	The epoxy coating received enhanced barrier/active inhibition capabilities with the addition of ZIF-67 and ZIF-67@APS.
5.	Epoxy [89]	Zeolitic imidazolate framework (ZIF-8)	Q235 carbon steel	3.5 wt.% NaCl solution	100 µm	8000 h	EIS, salt spray, adhesion test, oxygen permeability measurements	ZIF-8 is an active filler for epoxy resin that uses a chemical reaction to solve the filler/resin interface issue. ZIF-8 enhances the epoxy coating's mechanical qualities and long-term corrosion resistance.
6.	Epoxy [88]	Hollow mesoporous silica nanoparticles (HMSN) loaded with benzotriazole (BTA), subsequently modified with ZIF-8 (HMSN-BTA@ZIF-8 nanocontainers)	Q235 carbon steel	3.5 wt.% NaCl solution	52 ± 0.4 µm	30 days	EIS, salt spray, scanning kelvin probe technique	ZIF-8 served as a versatile gatekeeper for HMSN-BTA. Epoxy coatings made with HMSN-BTA@ZIF-8 demonstrated remarkable self-healing capability.
7.	Epoxy [93]	UIO-66, NH <sub>2</sub> -UIO, and NH <sub>2</sub> -UIO particles covalently functionalized by Glycidyl Methacrylate (GMA@NH <sub>2</sub> -UIO)	Mild steel	3.5 wt.% NaCl solution	85 µm	120 days	PDP, EIS, salt spray, pull-off, cathodic disbanding tests, DFT, and MD simulation	Terephthalic acid and 2-aminoterephthalic acid were used to create zirconium-based MOFs. It was demonstrated that the GMA@NH <sub>2</sub> -UIO filled epoxy coating has good barrier characteristics.
8.	Epoxy [98]	UIO-66 as the nanocontainer to encapsulate benzotriazole (BTA), then combined with graphene oxide (BTA-UIO-GO nanocomposite)	Carbon steel	3.5 wt.% NaCl solution	80 µm	30 days	EIS, oxygen permeability and water-uptake tests.	GO serves as a physical barrier and the initial line of defense for metal protection. The corrosion inhibitors are then released by the nanocontainers and absorbed on the corrosion sites to produce a layer that shields the metal. Then the UIO-66 will disintegrate in some alkaline environments, releasing more corrosion inhibitors.



Table 2. Cont.

S/N	Polymer Matrix	Fillers/Blends/Pigments	Metals/Alloys Coated	Corrosive Media	Coating Thickness	Immersion Time	Investigation Techniques	Findings/Remarks
9.	Epoxy [81]	Nanoceria-decorated cerium (III)-imidazole network (NC/CIN)	Mild steel	3.5 wt.% NaCl solution	$65 \pm 5 \mu\text{m}$	7 weeks	EIS, salt spray tests, dynamic mechanical, thermal analysis (DMTA)	The NC/CIN-contained epoxy demonstrated excellent barrier-inhibitive protective abilities. NC/CIN also significantly strengthened the cross-linking density and hardness of the epoxy coating.
10.	Epoxy [99]	Lanthanum-type metal-organic framework (La-MOF)	Mild steel	3.5 wt.% NaCl solution	between 90 and $100 \mu\text{m}$	12 weeks	EIS, PDP, salt spray, dry and wet adhesion tests	Even after being submerged in corrosive solutions for 12 weeks, the La-MOF-filled epoxy coating retained its barrier properties. According to adhesion experiments, including La-MOF nanoparticles increased epoxy adhesion by 15%.
11.	Epoxy [100]	Zeolitic imidazolate framework (ZIF)-derived layered double hydroxides (LDHs) as the gatekeepers for benzotriazole (BTA)-encapsulated mesoporous silica nanoparticles (MSNs-BTA). (MSNs-BTA@ZIF-LDHs nanocontainer)	Q235 steel	3.5 wt.% NaCl solution	$85 \pm 4 \mu\text{m}$	45 days	EIS, permeation experiments, salt spray tests, and the scanning vibrating electrode technique (SVET)	The micropores in the coating matrix were occluded by the evenly dispersed MSNs-BTA@ZIF-LDHs, limiting the corrosion medium's passage. The ion-exchange function of Ni-Co LDHs restricts the diffusion of $\text{Cl}^-$ , further lowering the concentration of $\text{Cl}^-$ at the coating-to-steel substrate interface. As corrosion activity increased in the later phases of immersion, the MSNs-BTA@ZIF-LDHs actively reacted to the local pH changes brought on by the corrosion process by releasing BTA corrosion inhibitors.
12.	Epoxy [90]	Dopamine-Metal Organic Frameworks (DA-MOFs)	Q235 steel	3.5 wt.% NaCl solution	$50 \pm 5 \mu\text{m}$	960 h	EIS, salt spray, pull-off adhesion tests	The performance of the waterborne epoxy coating was considerably enhanced by the DA-MOFs filler. As a result of the EIS test, it was discovered that the coating hinders the diffusion of charged ions to some extent, considerably enhancing MOF compatibility with the coatings.
13.	Epoxy [101]	Cu-MOF nanosheets based on Tetrakis(4-carboxyphenyl)porphyrin (Cu-TCPP MOFs)	Carbon steel	3.5 wt.% NaCl solution	$20 \pm 2 \mu\text{m}$	40 days	EIS, LEIS	The sample with Cu-TCPP nanosheets demonstrated a notable improvement in the protection properties compared to the controlled samples and bulk material.
14.	Epoxy [75]	MOF based on cerium (Ce-MOF) constructed on graphene oxide nanosheets (GO@Ce-MOF)	Mild steel	3.5 wt.% NaCl solution		7 weeks	EIS, salt spray tests	After 7 weeks of immersion in corrosive conditions, the GO@Ce-MOF/EP coating demonstrated exceptional barrier qualities with low-frequency values higher than $10^{10} \text{ cm}^2$ .
15.	Epoxy [97]	Silane-functionalized Cobalt-based MOF nanoparticles (ZIF-67@APS NPs)	Mild steel	3.5 wt.% NaCl solution	$50 \pm 5 \mu\text{m}$	50 days	EIS, salt spray, pull-off, and cathodic delamination tests.	ZIF-67@APS NPs could reduce the degree of steel corrosion inhibition by 81%. ZIF-67@APS NPs displayed exceptional anti-corrosion characteristics in an epoxy coating.

#### 4.2.5. Common Challenges Associated with the Use of MOFs in Polymer Coatings

Apart from the merits discussed on the applications of MOFs, some limitations exist in the use of MOFs in corrosion protection systems. Some MOFs have limited water stability and dispersion in the polymer matrix. Excellent water stability is essential for corrosion inhibition, water purification, solution phase catalysis, etc. However, some MOFs are reported to have good stability in water, and many MOFs materials are even used to remove contaminants from the water for long-term use. Commonly used MOFs series for this application include the University of Oslo (UiO) series, the Material of Institute Lavoisier (MIL) series, and Zeolitic Imidazolate Framework (ZIF) series substrates [102].

MOFs' agglomeration and dispersion problems usually occur at higher loading by conventional methods. The polymer particles can be prepared first in water, and then the MOF particles can be grown in situ. Matrimid polymers achieved a 40 wt.% loading without agglomeration by this method. Salman Shahid et al. [103] reported that instead of simply mixing and sonicating the polymer and the MOFs particles, the in-situ growth of the MOFs will result in excellent dispersion properties. Also, the particle fusion technique significantly increased the loading capacity of the polymer matrix with enhanced properties and without agglomeration of the particles. However, exceptional surface-active sites, abundant specific surface area, availability of easier preparation methods, various pore sizes, diverse topologies, and other corrosion inhibition benefits of MOFs are enough to rule out all the rectifiable limitations above.

### 5. Protection Design and Mechanisms of Polymer-Based Coating

The protection design and mechanism of polymer-based coating on steel can be based on the interaction of steel and coating at the metal-coating interface and/or the functionalization of coating. Haddadi and coworkers explain the interaction of steel and coating [104]. Chemical bonds are formed between matrices of coating and metallic substrates. At cathodic sites, the generation of  $\text{OH}^-$  accelerates the cathodic delamination of coating, sequel to the hydrolysis of chemical bonds formed. The generated  $\text{OH}^-$  groups can then react with  $\text{Fe}^{2+}$  produced by anodic reactions to obtain iron hydroxides. When different types of iron hydroxides/oxides accumulate in anodic sites, they lead to another pathway for the delamination of coatings.

By design, polymer-based coatings generally offer passive protection. However, researchers have explored several ways to improve the protection of metals by modifying coating formulations with organic and inorganic moieties, which harness unique mechanisms of protection to obtain coatings with fascinating barriers and active properties. This has resulted in polymeric coatings, which can be broadly categorized into (I) active protection coating, (II) self-healing coating, and (III) multifunctional coatings.

Polymer-based coatings with active protection are designed to accommodate active substances that, when released, hamper corrosion activities; thereby, offering protection to the underlying metal substrate [105,106]. Active substances can be directly trapped in polymer layers to obtain active protection. Yin et al. directly entrapped inhibitors inside an intrinsically conducting polymer, polypyrrole, to obtain a significant passivation effect—a result of the synergy between the effect of inhibitors (passivation of defect site and restoration of delaminated interface) and re-oxidation of polypyrrole [107]. In another work, cellulose nanofiber was grafted onto  $\text{Ti}_3\text{C}_2\text{T}_x$  ( $\text{Ti}_3\text{C}_2\text{T}_x\text{@CNF}$ ), then  $\text{Ti}_3\text{C}_2\text{T}_x\text{@CNF}$  nanohybrid was applied as nanofiller to endow epoxy coating with superior barrier property [108]. Electrochemical and corrosion product assessments indicated that incorporating  $\text{Ti}_3\text{C}_2\text{T}_x\text{@CNF}$  into epoxy significantly enhanced anti-corrosion performance.

Furthermore, Lutz and coworkers fabricated self-healing coatings such as the shape recovery polymer coating based on acrylated polycaprolactone polyurethanes and applied on hot dip galvanized steel [68]. The coating was shown to respond to temperature and close up an artificial defect; thereby, restoring the coating's corrosion protection and barrier properties. Liu et al. reported an intrinsic self-healing epoxy coating on Q235 steel substrate fabricated with 2-ureido-4[1H]-pyrimidinone (UPy) as a quadruple hydrogen

bonding unit, and grafted onto the backbones of an epoxy matrix by an amine-terminated oligo(propylene glycol) linker [109]. Introducing branched chain amines and UPy units improved the hydrogen bonding between the coating and the metal surface, increasing the adhesion strength. Self-healing capabilities combined with strong adhesion gave the coating significant protection.

Active protection systems with self-healing capabilities and other reactive properties/capabilities result in multifunctional coating protection [110–112]. Fu et al. integrated polycaprolactone (PCL) nanofiber with 2-mercaptobenzothiazole-loaded halloysite nanotubes (HNTs-MBT) and directly deposited on the surface of the metal substrate, resulting in an interconnected fiber network framework [113]. The authors achieved synergetic self-healing anti-corrosion performance by forming a self-assembly protective layer and repairing the coating passive barrier. The release of MBT is triggered by pH towards active protection. While coating defects are repaired by continuous polymer fiber upon heat treatment. Furthermore, through a simple facile design, self-healing, reprocess ability, and anti-corrosion have been reported in a multifunctional coating [114]. Haddadi et al. described a typical protection mechanism for an epoxy (EP) coating on mild steel aided by amino-functionalized MXene nanosheets doped with Ce (III) [104]. At prolonged immersion times, the corrosive electrolyte diffuses through the coating matrix at coating defect sites to reach the coating/metal interface. The defect region of MXene-Ce<sup>3+</sup>@EP coating proceeds to leach Ce<sup>3+</sup> from the Ti<sub>3</sub>C<sub>2</sub> MXene-Ce<sup>3+</sup> nanosheets. The leached Ce<sup>3+</sup> then deposits on the substrate in the scribed region, blocking cathodic sites and hampering the accessibility of electrolytes to metallic surfaces. Simultaneously, the unscribed region or intact area of coating with dispersed Ti<sub>3</sub>C<sub>2</sub> MXene-Ce<sup>3+</sup> nanosheets zigzags the electrolyte passage resulting in prolonged durability of the coating. In addition, Zhang et al. developed a new strategy to construct a triple functional filler by initially modifying basalt scales (Bt) using polydopamine (PDA) to introduce active sites, then followed by in situ grafting of molybdate-loaded, layered double hydroxide (molybdate-LDH) on the surface of PDA-modified basalt. The coating applied on carbon steel combined barrier properties, a chloride ion trapping effect, and a self-healing function to achieve long-term anti-corrosion performance [115].

However, introducing active carriers in polymer coating often compromises the integrity of the coating by creating pathways for water uptake. Water can potentially change the molecular structure of polymeric coatings and the mass transport of other permeants over time. The sorption mechanisms of polymer coatings may be affected by service conditions like temperature, humidity, or gas pressure. For example, as the epoxy network hydrates at high temperatures, the aggregate porosity within the coating increases [116]. Temperature effects are significant in most cases. In an investigation by Ha and Alfanzazi [117], it was observed that as the temperature rose from 20 to 80 °C, the coating's ohmic resistance was reduced by four orders of magnitude, and its capacitance nearly doubled.

## 6. Conclusions, Challenges, and Future Perspective

The harsh environments encountered by metallic materials in service are known to attack coated surfaces deteriorating the protective coverage. Influence on the effectiveness of the polymer-based coatings was summarized: of corrosion-inhibiting fillers, blends, and/or pigments; immersion time; and coating thickness. Coating design/formulation and adhesion are essential in deterring corrosion triggers as well as in the repair of exposed sites.

There are certain limitations and challenges to the use of polymer-based coatings. For instance, developing polymer coatings with desirable functions by incorporating additives may compromise the integrity of the coating. Often these additives create pathways for water uptake and sites for defect propagation. Furthermore, in most cases, introducing functionality may not be cost-effective; hence, hampering the possibility of some large-scale industrial applications. More so, some real application environments have harsh conditions making it difficult for the polymer-based coating to thrive. Generally, high effectiveness, long-term stability, durability, eco-friendliness, and large-scale application are among the

criteria that must be met for a coating to be considered technically viable. This is largely not always the case with polymer-based coating; hence, the need for continuous improvement.

Metal–organic frameworks as additives have vast applications and significance in polymer coating. A few advantages of using MOFs in polymer coatings for steel are improved mechanical properties, added functionality, improved corrosion protection, and increased thermal stability. Yet, issues still need to be resolved, such as the scalability of MOF synthesis, weak durability, unstable protection performance, poor adhesion, and the possibility of degradation over time. More study is required to fully grasp the potential of MOFs in polymer coatings and create useable solutions for their utilization. Moreover, it should be noted that theoretical study with computer simulations and machine learning will be very beneficial to fully understand the formation mechanism and structure characteristics of novel MOFs and their implications on polymer coating.

There is a huge potential for polymer-based coatings. The tunable properties of polymers offer the advantage of being harnessed for several applications. With researchers developing new ways of overcoming limitations, we envisage a generation of polymer-based coatings with fascinating properties and vast applications.

**Author Contributions:** Conceptualization, S.B.U. and T.P.D.R.; software, S.B.U. and I.I.U.; validation, S.B.U., I.I.U. and T.P.D.R.; writing—original draft preparation, S.B.U., R.P.R. and G.M.M.; writing—review and editing, S.B.U., R.P.R. and I.I.U.; visualization, S.B.U., R.P.R. and I.I.U.; supervision, T.P.D.R. All authors have read and agreed to the published version of the manuscript.

**Funding:** This research received no external funding.

**Data Availability Statement:** Not applicable.

**Acknowledgments:** Rajimol P. R. acknowledges UGC, India, for doctoral research fellowship.

**Conflicts of Interest:** The authors declare no conflict of interest.

## References

1. Hegedus, C.R. A holistic perspective of coatings technology. *JCT Res.* **2004**, *1*, 5–20.
2. Verkholtantsev, V.V. Functional variety: Effects and properties in surface-functional coating systems. *Eur. Coat. J.* **2003**, *9*, 18–25.
3. Montemor, M.F. Functional and smart coatings for corrosion protection: A review of recent advances. *Surf. Coat. Technol.* **2014**, *258*, 17–37. [[CrossRef](#)]
4. Serednyts'kyi, Y.A. Polyurethane materials as anticorrosive coatings of pipelines. *Mater. Sci.* **2000**, *36*, 415–421. [[CrossRef](#)]
5. Kalaivani, R.; Arasu, P.T.; Rajendran, S. Corrosion inhibition by polymers—A bird's eyeview. *Eur. Chem. Bull.* **2013**, *2*, 807–815.
6. Álvarez-Paino, M.; Muñoz-Bonilla, A.; Fernández-García, M. Antimicrobial polymers in the nano-world. *Nanomaterials* **2017**, *7*, 48. [[CrossRef](#)]
7. Zhou, H.C.; Long, J.R.; Yaghi, O.M. Introduction to metal–organic frameworks. *Chem. Rev.* **2012**, *112*, 673–674. [[CrossRef](#)]
8. Mahmoodi, N.M.; Taghizadeh, M.; Taghizadeh, A.; Abdi, J.; Hayati, B.; Shekarchi, A.A. Bio-based magnetic metal-organic framework nanocomposite: Ultrasound-assisted synthesis and pollutant (heavy metal and dye) removal from aqueous media. *Appl. Surf. Sci.* **2019**, *480*, 288–299. [[CrossRef](#)]
9. Liu, X.; Yue, T.; Qi, K.; Xia, B.Y.; Chen, Z.; Qiu, Y.; Guo, X. Probe into metal-organic framework membranes fabricated via versatile polydopamine-assisted approach onto metal surfaces as anticorrosion coatings. *Corros. Sci.* **2020**, *177*, 108949. [[CrossRef](#)]
10. Mahmoodi, N.M.; Oveisi, M.; Taghizadeh, A.; Taghizadeh, M. Synthesis of pearl necklace-like ZIF-8@chitosan/PVA nanofiber with synergistic effect for recycling aqueous dye removal. *Carbohydr. Polym.* **2020**, *227*, 115364. [[CrossRef](#)]
11. Zhou, Z.; Xing, X.; Tian, C.; Wei, W.; Li, D.; Hu, F.; Du, S. A multifunctional nanocage-based MOF with tri- and tetranuclear zinc cluster secondary building units. *Sci. Rep.* **2018**, *8*, 3117. [[CrossRef](#)] [[PubMed](#)]
12. Bao, Y.; Chen, Y.; Lim, T.-T.; Wang, R.; Hu, X. A novel metal–organic framework (MOF)–mediated interfacial polymerization for direct deposition of polyamide layer on ceramic substrates for nanofiltration. *Adv. Mater. Interfaces* **2019**, *6*, 1900132. [[CrossRef](#)]
13. Lu, X.F.; Fang, Y.; Luan, D.; Lou, X.W.D. Metal–organic frameworks derived functional materials for electrochemical energy storage and conversion: A mini review. *Nano Lett.* **2021**, *21*, 1555–1565. [[CrossRef](#)]
14. Ding, Z.; Wang, C.; Wang, S.; Wu, L.; Zhang, X. Light-harvesting metal-organic framework nanopores for ratiometric fluorescence energy transfer-based determination of pH values and temperature. *Microchim. Acta* **2019**, *186*, 476. [[CrossRef](#)]
15. So, M.C.; Wiederrecht, G.P.; Mondloch, J.E.; Hupp, J.T.; Farha, O.K. Metal–organic framework materials for light-harvesting and energy transfer. *Chem. Commun.* **2015**, *51*, 3501–3510. [[CrossRef](#)]
16. Rout, T.; Jha, G.; Singh, A.; Bandyopadhyay, N.; Mohanty, O. Development of conducting polyaniline coating: A novel approach to superior corrosion resistance. *Surf. Coat. Technol.* **2003**, *167*, 16–24. [[CrossRef](#)]

17. Wessling, B.; Posdorfer, J. Nanostructures of the dispersed organic metal polyaniline responsible for macroscopic effects in corrosion protection. *Synth. Met.* **1999**, *102*, 1400–1401. [\[CrossRef\]](#)
18. Goswami, R.N.; Mourya, P.; Behera, B.; Khatri, O.P.; Ray, A. Graphene-polyaniline nanocomposite based coatings: Role of convertible forms of polyaniline to mitigate steel corrosion. *Appl. Surf. Sci.* **2022**, *599*, 153939. [\[CrossRef\]](#)
19. Garcia, B.; Lamzoudi, A.; Pillier, F.; Nguyen, H.; Le, T.; Deslouis, C. Oxide/polypyrrole composite films for corrosion protection of iron. *J. Electrochem. Soc.* **2022**, *149*, B560. [\[CrossRef\]](#)
20. Yeh, J.-M.; Chin, C.-P. Structure and properties of poly(o-methoxyaniline)–clay nanocomposite materials. *J. Appl. Polym. Sci.* **2003**, *88*, 1072–1080. [\[CrossRef\]](#)
21. Tatiya, P.D.; Hedao, R.K.; Mahulikar, P.P.; Gite, V.V. Novel polyurea microcapsules using dendritic functional monomer: Synthesis, characterization, and its use in self-healing and anticorrosive polyurethane coatings. *Ind. Eng. Chem. Res.* **2013**, *52*, 1562–1570. [\[CrossRef\]](#)
22. Huang, T.-C.; Lai, G.-H.; Li, C.-E.; Tsai, M.-H.; Wang, P.-Y.; Chung, Y.-H.; Lin, M.-H. Correction: Advanced anti-corrosion coatings prepared from  $\alpha$ -zirconium phosphate/polyurethane nanocomposites. *RSC Adv.* **2017**, *7*, 22540. [\[CrossRef\]](#)
23. Wan, T.; Chen, D. Synthesis and properties of self-healing waterborne polyurethanes containing disulfide bonds in the main chain. *J. Mater. Sci.* **2017**, *52*, 197–207. [\[CrossRef\]](#)
24. Michael, S. Basic concepts in polyurethane chemistry and technology. In *Szycher's Handbook of Polyurethanes*; CRC Press: Boca Raton, FL, USA, 2012.
25. Ghosh, B.; Urban, M.W. Self-repairing oxetane-substituted chitosan polyurethane networks. *Science* **2009**, *323*, 1458–1460. [\[CrossRef\]](#)
26. Chaudhari, A.B.; Tatiya, P.D.; Hedao, R.K.; Kulkarni, R.D.; Gite, V.V. Polyurethane prepared from neem oil polyesteramides for self-healing anticorrosive coatings. *Ind. Eng. Chem. Res.* **2013**, *52*, 10189–10197. [\[CrossRef\]](#)
27. Marathe, R.; Tatiya, P.; Chaudhari, A.; Lee, J.; Mahulikar, P.; Sohn, D.; Gite, V. Neem acetylated polyester polyol—Renewable source based smart PU coatings containing quinoline (corrosion inhibitor) encapsulated polyurea microcapsules for enhance anticorrosive property. *Ind. Crops Prod.* **2015**, *77*, 239–250. [\[CrossRef\]](#)
28. Pourhashem, S.; Vaezi, M.R.; Rashidi, A.; Bagherzadeh, M.R. Distinctive roles of silane coupling agents on the corrosion inhibition performance of graphene oxide in epoxy coatings. *Prog. Org. Coat.* **2017**, *111*, 47–56. [\[CrossRef\]](#)
29. Ellis, B. Introduction to the chemistry, synthesis, manufacture and characterization of epoxy resins. In *Chemistry and Technology of Epoxy Resins*; Ellis, B., Ed.; Springer: Dordrecht, The Netherlands, 1993; pp. 1–36.
30. Boyle, M.A.; Martin, C.J.; Neuner, J.D. Epoxy Resins. In *Composites*; Miracle, D.B., Donaldson, S.L., Eds.; ASM International: Almere, The Netherlands, 2001.
31. Hang, T.T.X.; Truc, T.A.; Olivier, M.-G.; Vandermiers, C.; Guérit, N.; Pébère, N. Corrosion protection mechanisms of carbon steel by an epoxy resin containing indole-3 butyric acid modified clay. *Prog. Org. Coat.* **2010**, *69*, 410–416. [\[CrossRef\]](#)
32. Manjumeena, R.; Venkatesan, R.; Duraibabu, D.; Sudha, J.; Rajendran, N.; Kalaichelvan, P.T. Green nanosilver as reinforcing eco-friendly additive to epoxy coating for augmented anticorrosive and antimicrobial behavior. *Silicon* **2016**, *8*, 277–298. [\[CrossRef\]](#)
33. Njoku, D.I.; Cui, M.; Xiao, H.; Shang, B.; Li, Y. Understanding the anticorrosive protective mechanisms of modified epoxy coatings with improved barrier, active and self-healing functionalities: EIS and spectroscopic techniques. *Sci. Rep.* **2017**, *7*, 15597. [\[CrossRef\]](#)
34. Qian, B.; Song, Z.; Hao, L.; Wang, W.; Kong, D. Self-healing epoxy coatings based on nanocontainers for corrosion protection of mild steel. *J. Electrochem. Soc.* **2017**, *164*, C54–C60. [\[CrossRef\]](#)
35. Haghayegh, M.; Mirabedini, S.M.; Yeganeh, H. Microcapsules containing multi-functional reactive isocyanate-terminated polyurethane prepolymer as a healing agent. Part 1: Synthesis and optimization of reaction conditions. *J. Mater. Sci.* **2016**, *51*, 3056–3068. [\[CrossRef\]](#)
36. Liu, D.; Zhao, W.; Liu, S.; Cen, Q.; Xue, Q. In situ regulating of surface morphologies, anti-corrosion and tribological properties of epoxy resin coatings by heat treatment. *Surf. Topogr. Metrol. Prop.* **2017**, *5*, 024003. [\[CrossRef\]](#)
37. Wang, N.; Diao, X.; Zhang, J.; Kang, P. Corrosion resistance of waterborne epoxy coatings by incorporation of dopamine treated mesoporous-TiO<sub>2</sub> particles. *Coatings* **2018**, *8*, 209. [\[CrossRef\]](#)
38. Samad, U.A.; Alam, M.A.; Sherif, E.-S.M.; Alam, M.; Shaikh, H.; Alharthi, N.H.; Al-Zahrani, S.M. Synergistic Effect of Ag and ZnO Nanoparticles on Polypyrrole-Incorporated Epoxy/2pack Coatings and Their Corrosion Performances in Chloride Solutions. *Coatings* **2019**, *9*, 287. [\[CrossRef\]](#)
39. Keyvani, A.; Yeganeh, M.; Rezaeyan, H. Application of mesoporous silica nanocontainers as an intelligent host of molybdate corrosion inhibitor embedded in the epoxy coated steel. *Prog. Nat. Sci. Mater. Int.* **2017**, *27*, 261–267. [\[CrossRef\]](#)
40. Chopra, I.; Ola, S.K.; Priyanka; Dhayal, V.; Shekhawat, D.S. Recent advances in epoxy coatings for corrosion protection of steel: Experimental and modelling approach—A review. *Mater. Today Proc.* **2022**, *62*, 1658–1663. [\[CrossRef\]](#)
41. Yu, Z.; Di, H.; Ma, Y.; He, Y.; Liang, L.; Lv, L.; Ran, X.; Pan, Y.; Luo, Z. Preparation of graphene oxide modified by titanium dioxide to enhance the anti-corrosion performance of epoxy coatings. *Surf. Coat. Technol.* **2015**, *276*, 471–478. [\[CrossRef\]](#)
42. Nair, L.S.; Laurencin, C.T. Biodegradable polymers as biomaterials. *Prog. Polym. Sci.* **2007**, *32*, 762–798. [\[CrossRef\]](#)
43. Karak, N. 15—Biopolymers for paints and surface coatings. In *Biopolymers and Biotech Admixtures for Eco-Efficient Construction Materials*; Pacheco-Torgal, F., Ivanov, V., Karak, N., Jonkers, H., Eds.; Woodhead Publishing: Sawston, UK, 2016; pp. 333–368.



44. Dastpak, A.; Hannula, P.-M.; Lundström, M.; Wilson, B.P. A sustainable two-layer lignin-anodized composite coating for the corrosion protection of high-strength low-alloy steel. *Prog. Org. Coat.* **2020**, *148*, 105866. [\[CrossRef\]](#)
45. Zulkifli, F.; Ali, N.; Yusof, M.S.M.; Isa, M.; Yabuki, A.; Nik, W.W. Henna leaves extract as a corrosion inhibitor in acrylic resin coating. *Prog. Org. Coat.* **2017**, *105*, 310–319. [\[CrossRef\]](#)
46. Qian, B.; Michailidis, M.; Bilton, M.; Hobson, T.; Zheng, Z.; Shchukin, D. Tannic complexes coated nanocontainers for controlled release of corrosion inhibitors in self-healing coatings. *Electrochim. Acta* **2019**, *297*, 1035–1041. [\[CrossRef\]](#)
47. Seidi, F.; Crespy, D. Fighting corrosion with stimuli-responsive polymer conjugates. *Chem. Commun.* **2020**, *56*, 11931–11940. [\[CrossRef\]](#) [\[PubMed\]](#)
48. Hochmannová, L. Combination well done: Zinc rich primers with micaceous iron oxide. *Eur. Coat. J.* **2003**, *9*, 26–32.
49. Yeh, J.-M.; Liou, S.-J.; Lin, C.-G.; Chang, Y.-P.; Yu, Y.-H.; Cheng, C.-F. Effective enhancement of anticorrosive properties of polystyrene by polystyrene-clay nanocomposite materials. *J. Appl. Polym. Sci.* **2004**, *92*, 1970–1976. [\[CrossRef\]](#)
50. Mills, D.J.; Jamali, S.S. The best tests for anti-corrosive paints. And why: A personal viewpoint. *Prog. Org. Coat.* **2017**, *102*, 8–17. [\[CrossRef\]](#)
51. Wang, L.; Deng, L.; Zhang, D.; Qian, H.; Du, C.; Li, X.; Mol, J.M.; Terryn, H.A. Shape memory composite (SMC) self-healing coatings for corrosion protection. *Prog. Org. Coat.* **2016**, *97*, 261–268. [\[CrossRef\]](#)
52. Moradi, M.; Yeganeh, H.; Pazokifard, S. Synthesis and assessment of novel anticorrosive polyurethane coatings containing an amine-functionalized nanoclay additive prepared by the cathodic electrophoretic deposition method. *RSC Adv.* **2016**, *6*, 28089–28102. [\[CrossRef\]](#)
53. Falcón, J.; Batista, F.; Aoki, I. Encapsulation of dodecylamine corrosion inhibitor on silica nanoparticles. *Electrochim. Acta* **2014**, *124*, 109–118. [\[CrossRef\]](#)
54. Atta, A.M.; Al-Hodan, H.A.; Hameed, R.S.A.; Ezzat, A.O. Preparation of green cardanol-based epoxy and hardener as primer coatings for petroleum and gas steel in marine environment. *Prog. Org. Coat.* **2017**, *111*, 283–293. [\[CrossRef\]](#)
55. Behzadnasab, M.; Mirabedini, S.; Kabiri, K.; Jamali, S. Corrosion performance of epoxy coatings containing silane treated ZrO<sub>2</sub> nanoparticles on mild steel in 3.5% NaCl solution. *Corros. Sci.* **2011**, *53*, 89–98. [\[CrossRef\]](#)
56. Sanaei, Z.; Ramezanzadeh, B.; Shahrabi, T. Anti-corrosion performance of an epoxy ester coating filled with a new generation of hybrid green organic/inorganic inhibitive pigment; electrochemical and surface characterizations. *Appl. Surf. Sci.* **2018**, *454*, 1–15. [\[CrossRef\]](#)
57. Lutz, A.; Berg, O.V.D.; Wielant, J.; De Graeve, I.; Terryn, H. A multiple-action self-healing coating. *Front. Mater.* **2016**, *2*, 73. [\[CrossRef\]](#)
58. Tran, T.H.; Vimalanandan, A.; Genchev, G.; Fickert, J.; Landfester, K.; Crespy, D.; Rohwerder, M. Regenerative nano-hybrid coating tailored for autonomous corrosion protection. *Adv. Mater.* **2015**, *27*, 3825–3830. [\[CrossRef\]](#) [\[PubMed\]](#)
59. Wang, W.; Li, W.; Song, L.; Fan, W.; Xiong, C.; Gao, X.; Zhang, X.; Liu, X. Self-healing performance of coatings containing synthetic hexamethylene diisocyanate biuret microcapsules. *J. Electrochem. Soc.* **2017**, *164*, C635–C640. [\[CrossRef\]](#)
60. Ahmed, R.A.; Farghali, R.A.; Fekry, A.M. Study for the Stability and Corrosion Inhibition of Electrophoretic Deposited Chitosan on Mild Steel Alloy in Acidic Medium. *Int. J. Electrochem. Sci.* **2012**, *7*, 7270–7282.
61. Baldissera, A.; Ferreira, C. Coatings based on electronic conducting polymers for corrosion protection of metals. *Prog. Org. Coat.* **2012**, *75*, 241–247. [\[CrossRef\]](#)
62. Sonawane, S.; Bhanvase, B.; Jamali, A.; Dubey, S.; Kale, S.; Pinjari, D.V.; Kulkarni, R.; Gogate, P.; Pandit, A. Improved active anticorrosion coatings using layer-by-layer assembled ZnO nanocontainers with benzotriazole. *Chem. Eng. J.* **2012**, *189–190*, 464–472. [\[CrossRef\]](#)
63. Rawat, N.K.; Sinha, A.K.; Ahmad, S. Conducting poly(o-anisidine-co-o-phenyldiamine) nanorod dispersed epoxy composite coatings: Synthesis, characterization and corrosion protective performance. *RSC Adv.* **2015**, *5*, 94933–94948. [\[CrossRef\]](#)
64. Cho, S.H.; White, S.R.; Braun, P.V. Self-Healing Polymer Coatings. *Adv. Mater.* **2009**, *21*, 645–649. [\[CrossRef\]](#)
65. Falcón, J.M.; Sawczen, T.; Aoki, I.V. Dodecylamine-loaded halloysite nanocontainers for active anticorrosion coatings. *Front. Mater.* **2015**, *2*, 69. [\[CrossRef\]](#)
66. Patil, C.K.; Jirimali, H.D.; Mahajan, M.; Paradeshi, J.S.; Chaudhari, B.L.; Gite, V.V. Functional anti-corrosive and anti-bacterial surface coatings based on mercaptosuccinic and thiodipropionic acids and algae oil as renewable feedstock. *React. Funct. Polym.* **2019**, *139*, 142–152. [\[CrossRef\]](#)
67. Rahman, O.U.; Bhat, S.I.; Yu, H.; Ahmad, S. Hyperbranched soya alkyd nanocomposite: A sustainable feedstock-based anticorrosive nanocomposite coatings. *ACS Sustain. Chem. Eng.* **2017**, *5*, 9725–9734. [\[CrossRef\]](#)
68. Lutz, A.; van den Berg, O.; Van Damme, J.; Verheyen, K.; Bauters, E.; De Graeve, I.; Du Prez, F.E.; Terryn, H. A shape-recovery polymer coating for the corrosion protection of metallic surfaces. *ACS Appl. Mater. Interfaces* **2015**, *7*, 175–183. [\[CrossRef\]](#) [\[PubMed\]](#)
69. Viveros, S.; Menchaca, C.; Hernández, M.; Covelo, A.; Uruchurtu, J. Recycled ABS polymer doped with outdated lansoprazole as a corrosion protection composite coating for mild steel in chloride solution. *Eur. J. Eng. Res. Sci.* **2020**, *5*, 429–435. [\[CrossRef\]](#)
70. Ramesh, M.; Deepa, C. Chapter 1—Metal-organic frameworks and their composites. In *Metal-Organic Frameworks for Chemical Reactions*; Khan, A., Verpoort, F., Asiri, A.M., Hoque, M.E., Bilgrami, A.L., Azam, M., Naidu, K.C.B., Eds.; Elsevier: Amsterdam, The Netherlands, 2021; pp. 1–18.

71. Ramezanzadeh, M.; Ramezanzadeh, B. Chapter 12—Thermomechanical and anticorrosion characteristics of metal-organic frameworks. In *Metal-Organic Frameworks for Chemical Reactions*; Khan, A., Verpoort, F., Asiri, A.M., Hoque, M.E., Bilgrami, A.L., Azam, M., Naidu, K.C.B., Eds.; Elsevier: Amsterdam, The Netherlands, 2021; pp. 295–330.
72. Morozan, A.; Jaouen, F. Metal organic frameworks for electrochemical applications. *Energy Environ. Sci.* **2012**, *5*, 9269–9290. [\[CrossRef\]](#)
73. Zhao, Y.; Jiang, F.; Chen, Y.-Q.; Hu, J.-M. Coatings embedded with GO/MOFs nanocontainers having both active and passive protecting properties. *Corros. Sci.* **2020**, *168*, 108563. [\[CrossRef\]](#)
74. Etaiw, S.E.-d.H.; Fouda, A.E.-A.S.; Abdou, S.N.; El-Bendary, M.M. Structure, characterization and inhibition activity of new metal-organic framework. *Corros. Sci.* **2011**, *53*, 3657–3665. [\[CrossRef\]](#)
75. Keshmiri, N.; Najmi, P.; Ramezanzadeh, M.; Ramezanzadeh, B. Designing an eco-friendly lanthanide-based metal organic framework (MOF) assembled graphene-oxide with superior active anti-corrosion performance in epoxy composite. *J. Clean. Prod.* **2021**, *319*, 128732. [\[CrossRef\]](#)
76. Tian, H.; Li, W.; Liu, A.; Gao, X.; Han, P.; Ding, R.; Yang, C.; Wang, D. Controlled delivery of multi-substituted triazole by metal-organic framework for efficient inhibition of mild steel corrosion in neutral chloride solution. *Corros. Sci.* **2018**, *131*, 1–16. [\[CrossRef\]](#)
77. Li, W.-J.; Ren, B.-H.; Chen, Y.; Wang, X.; Cao, R. Excellent efficacy of MOF films for bronze artwork conservation: The key role of HKUST-1 film nanocontainers in selectively positioning and protecting inhibitors. *ACS Appl. Mater. Interfaces* **2018**, *10*, 37529–37534. [\[CrossRef\]](#)
78. Etaiw, S.E.-d.H.; Fouda, A.E.-A.S.; Amer, S.A.; El-Bendary, M.M. Structure, characterization and anti-corrosion activity of the new metal-organic framework [Ag(qox)(4-ab)]. *J. Inorg. Organomet. Polym. Mater.* **2011**, *21*, 327–335. [\[CrossRef\]](#)
79. Lin, Y.-T.; Don, T.-M.; Wong, C.-J.; Meng, F.-C.; Lin, Y.-J.; Lee, S.-Y.; Lee, C.-F.; Chiu, W.-Y. Improvement of mechanical properties and anticorrosion performance of epoxy coatings by the introduction of polyaniline/graphene composite. *Surf. Coat. Technol.* **2019**, *374*, 1128–1138. [\[CrossRef\]](#)
80. Shi, X.; Nguyen, T.A.; Suo, Z.; Liu, Y.; Avci, R. Effect of nanoparticles on the anticorrosion and mechanical properties of epoxy coating. *Surf. Coat. Technol.* **2009**, *204*, 237–245. [\[CrossRef\]](#)
81. Motamedi, M.H.K.; Ramezanzadeh, M.; Ramezanzadeh, B.; Mahdavian, M. One-pot synthesis and construction of a high performance metal-organic structured nano pigment based on nanoceria decorated cerium (III)-imidazole network (NC/CIN) for effective epoxy composite coating anti-corrosion and thermo-mechanical properties improvement. *Chem. Eng. J.* **2020**, *382*, 122820.
82. Tang, Y.; Tanase, S. Water-alcohol adsorptive separations using metal-organic frameworks and their composites as adsorbents. *Microporous Mesoporous Mater.* **2020**, *295*, 109946. [\[CrossRef\]](#)
83. Yeganeh, M.; Keyvani, A. The effect of mesoporous silica nanocontainers incorporation on the corrosion behavior of scratched polymer coatings. *Prog. Org. Coat.* **2016**, *90*, 296–303. [\[CrossRef\]](#)
84. Su, L.; Li, Y.; Liu, Y.; Ma, R.; Liu, Y.; Huang, F.; An, Y.; Ren, Y.; van der Mei, H.C.; Busscher, H.J.; et al. Antifungal-inbuilt metal-organic-frameworks eradicate *Candida albicans* biofilms. *Adv. Funct. Mater.* **2020**, *30*, 2000537. [\[CrossRef\]](#)
85. Li, H.; Qiang, Y.; Zhao, W.; Zhang, S. 2-Mercaptobenzimidazole-inbuilt metal-organic-frameworks modified graphene oxide towards intelligent and excellent anti-corrosion coating. *Corros. Sci.* **2021**, *191*, 109715. [\[CrossRef\]](#)
86. Ramezanzadeh, M.; Ramezanzadeh, B.; Mahdavian, M.; Bahlakeh, G. Development of metal-organic framework (MOF) decorated graphene oxide nanoplateforms for anti-corrosion epoxy coatings. *Carbon* **2020**, *161*, 231–251. [\[CrossRef\]](#)
87. Ren, B.; Chen, Y.; Li, Y.; Li, W.; Gao, S.; Li, H.; Cao, R. Rational design of metallic anti-corrosion coatings based on zinc gluconate@ZIF-8. *Chem. Eng. J.* **2020**, *384*, 123389. [\[CrossRef\]](#)
88. Zhou, C.; Li, Z.; Li, J.; Yuan, T.; Chen, B.; Ma, X.; Jiang, D.; Luo, X.; Chen, D.; Liu, Y. Epoxy composite coating with excellent anticorrosion and self-healing performances based on multifunctional zeolitic imidazolate framework derived nanocontainers. *Chem. Eng. J.* **2020**, *385*, 123835. [\[CrossRef\]](#)
89. Duan, S.; Dou, B.; Lin, X.; Zhao, S.; Emori, W.; Pan, J.; Hu, H.; Xiao, H. Influence of active nanofiller ZIF-8 metal-organic framework (MOF) by microemulsion method on anticorrosion of epoxy coatings. *Colloids Surf. A Physicochem. Eng. Asp.* **2021**, *624*, 126836. [\[CrossRef\]](#)
90. Wang, N.; Zhang, Y.; Chen, J.; Zhang, J.; Fang, Q. Dopamine modified metal-organic frameworks on anti-corrosion properties of waterborne epoxy coatings. *Prog. Org. Coat.* **2017**, *109*, 126–134. [\[CrossRef\]](#)
91. Lashgari, S.M.; Yari, H.; Mahdavian, M.; Ramezanzadeh, B.; Bahlakeh, G.; Ramezanzadeh, M. Synthesis of graphene oxide nanosheets decorated by nanoporous zeolite-imidazole (ZIF-67) based metal-organic framework with controlled-release corrosion inhibitor performance: Experimental and detailed DFT-D theoretical explorations. *J. Hazard. Mater.* **2021**, *404*, 124068. [\[CrossRef\]](#)
92. Guo, Y.; Wang, J.; Zhang, D.; Qi, T.; Li, G.L. pH-responsive self-healing anticorrosion coatings based on benzotriazole-containing zeolitic imidazole framework. *Colloids Surf. A Physicochem. Eng. Asp.* **2019**, *561*, 1–8. [\[CrossRef\]](#)
93. Ramezanzadeh, M.; Ramezanzadeh, B.; Bahlakeh, G.; Tati, A.; Mahdavian, M. Development of an active/barrier bi-functional anti-corrosion system based on the epoxy nanocomposite loaded with highly-coordinated functionalized zirconium-based nanoporous metal-organic framework (Zr-MOF). *Chem. Eng. J.* **2021**, *408*, 127361. [\[CrossRef\]](#)
94. Alipanah, N.; Yari, H.; Mahdavian, M.; Ramezanzadeh, B.; Bahlakeh, G. MIL-88A (Fe) filler with duplicate corrosion inhibitive/barrier effect for epoxy coatings: Electrochemical, molecular simulation, and cathodic delamination studies. *J. Ind. Eng. Chem.* **2021**, *97*, 200–215. [\[CrossRef\]](#)

95. Abdi, J.; Izadi, M.; Bozorg, M. Improvement of anti-corrosion performance of an epoxy coating using hybrid UiO-66-NH<sub>2</sub>/carbon nanotubes nanocomposite. *Sci. Rep.* **2022**, *12*, 10660. [\[CrossRef\]](#)
96. Ghohrodi, A.R.; Ramezanzadeh, M.; Ramezanzadeh, B. Investigating the thermo-mechanical and UV-shielding properties of a nano-porous Zr(IV)-type metal-organic framework (MOF) incorporated epoxy composite coating. *Prog. Org. Coat.* **2022**, *164*, 106693. [\[CrossRef\]](#)
97. Lashgari, S.M.; Yari, H.; Mahdavian, M.; Ramezanzadeh, B.; Bahlakeh, G.; Ramezanzadeh, M. Application of nanoporous cobalt-based ZIF-67 metal-organic framework (MOF) for construction of an epoxy-composite coating with superior anti-corrosion properties. *Corros. Sci.* **2021**, *178*, 109099. [\[CrossRef\]](#)
98. Chen, H.; Yu, Z.; Cao, K.; Chen, L.; Pang, Y.; Xie, C.; Jiang, Y.; Zhu, L.; Wang, J. Preparation of a BTA-UIO-GO nanocomposite to endow coating systems with active inhibition and passive anticorrosion performances. *New J. Chem.* **2021**, *45*, 16069–16082. [\[CrossRef\]](#)
99. Keramatinia, M.; Majidi, R.; Ramezanzadeh, B. La-MOF coordination polymer: An effective environmentally friendly pH-sensitive corrosion inhibitive-barrier nanofiller for the epoxy polyamide coating reinforcement. *J. Environ. Chem. Eng.* **2022**, *10*, 108246. [\[CrossRef\]](#)
100. Zhou, C.; Zhang, H.; Pan, X.; Li, J.; Chen, B.; Gong, W.; Yang, Q.; Luo, X.; Zeng, H.; Liu, Y. Smart waterborne composite coating with passive/active protective performances using nanocontainers based on metal organic frameworks derived layered double hydroxides. *J. Colloid Interface Sci.* **2022**, *619*, 132–147. [\[CrossRef\]](#)
101. Qiu, S.; Su, Y.; Zhao, H.; Wang, L.; Xue, Q. Ultrathin metal-organic framework nanosheets prepared via surfactant-assisted method and exhibition of enhanced anticorrosion for composite coatings. *Corros. Sci.* **2021**, *178*, 109090. [\[CrossRef\]](#)
102. Zhang, S.; Wang, J.; Zhang, Y.; Ma, J.; Huang, L.; Yu, S.; Chen, L.; Song, G.; Qiu, M.; Wang, X. Applications of water-stable metal-organic frameworks in the removal of water pollutants: A review. *Environ. Pollut.* **2021**, *291*, 118076. [\[CrossRef\]](#) [\[PubMed\]](#)
103. Shahid, S.; Nijmeijer, K.; Nehache, S.; Vankelecom, I.; Deratani, A.; Quemener, D. MOF-mixed matrix membranes: Precise dispersion of MOF particles with better compatibility via a particle fusion approach for enhanced gas separation properties. *J. Membr. Sci.* **2015**, *492*, 21–31. [\[CrossRef\]](#)
104. Haddadi, S.A.; Hu, S.; Ghaderi, S.; Ghanbari, A.; Ahmadipour, M.; Pung, S.-Y.; Li, S.; Feilizadeh, M.; Arjmand, M. Amino-Functionalized MXene Nanosheets Doped with Ce(III) as Potent Nanocontainers toward Self-Healing Epoxy Nanocomposite Coating for Corrosion Protection of Mild Steel. *ACS Appl. Mater. Interfaces* **2021**, *13*, 42074–42093. [\[CrossRef\]](#) [\[PubMed\]](#)
105. Kobzar, Y.L.; Fatyeyeva, K. Ionic liquids as green and sustainable steel corrosion inhibitors: Recent developments. *J. Chem. Eng.* **2021**, *425*, 131480. [\[CrossRef\]](#)
106. Yan, D.; Zhang, Z.; Zhang, W.; Wang, Y.; Zhang, M.; Zhang, T.; Wang, J. Smart self-healing coating based on the highly dispersed silica/carbon nanotube nanomaterial for corrosion protection of steel. *Prog. Org. Coat.* **2022**, *164*, 106694. [\[CrossRef\]](#)
107. Yin, Y.; Prabhakar, M.; Ebbinghaus, P.; Corrêa da Silva, C.; Rohwerder, M. Neutral inhibitor molecules entrapped into polypyrrole network for corrosion protection. *Chem. Eng. J.* **2022**, *440*, 135739. [\[CrossRef\]](#)
108. Wu, Y.; Zhao, W.; Liu, S.; Wang, L. Ti3C2Tx@CNF nanohybrid improving the corrosion resistance of waterborne epoxy coating under 15 MPa alternating hydrostatic pressure. *Chem. Eng. J.* **2022**, *438*, 135483. [\[CrossRef\]](#)
109. Liu, T.; Zhao, H.; Zhang, D.; Lou, Y.; Huang, L.; Ma, L.; Hao, X.; Dong, L.; Rosei, F.; Lau, W.M. Ultrafast and high-efficient self-healing epoxy coatings with active multiple hydrogen bonds for corrosion protection. *Corros. Sci.* **2021**, *187*, 109485. [\[CrossRef\]](#)
110. Fadl, A.; Abdou, M.; Zordok, W.; Sadeek, S. Intrinsic anti-corrosion, self-healing and mechanical resistance behaviors of epoxy composite coating intercalated with novel mixed Ni(II), Pd(II), and Cd(II) complex cross-linking accelerators for steel petroleum tanks. *J. Mater. Res. Technol.* **2021**, *15*, 2242–2275. [\[CrossRef\]](#)
111. Li, C.; Wang, P.; Zhang, D. Multifunctional and robust composite coating with water repellency and self-healing against marine corrosion. *Ind. Eng. Chem. Res.* **2022**, *110*, 529–541. [\[CrossRef\]](#)
112. Wang, J.; Ma, L.; Guo, X.; Wu, S.; Liu, T.; Yang, J.; Ren, C.; Li, S.; Zhang, D. Two birds with one stone: Nanocontainers with synergetic inhibition and corrosion sensing abilities towards intelligent self-healing and self-reporting coating. *Chem. Eng. J.* **2022**, *433*, 134515. [\[CrossRef\]](#)
113. Fu, X.; Du, W.; Dou, H.; Fan, Y.; Xu, J.; Tian, L.; Zhao, J.; Ren, L. Nanofiber composite coating with self-healing and active anticorrosive performances. *ACS Appl. Mater. Interfaces* **2021**, *13*, 57880–57892. [\[CrossRef\]](#)
114. Mo, R.; Hu, J.; Huang, H.; Sheng, X.; Zhang, X. Tunable, self-healing and corrosion inhibiting dynamic epoxy-polyimine network built by post-crosslinking. *J. Mater. Chem. A* **2019**, *7*, 3031–3038. [\[CrossRef\]](#)
115. Zhang, M.; Xu, F.; Lin, D.; Peng, J.; Zhu, Y.; Wang, H. A smart anti-corrosion coating based on triple functional fillers. *Chem. Eng. J.* **2022**, *446*, 137078. [\[CrossRef\]](#)

116. Zargarnezhad, H.; Asselin, E.; Wong, D.; Lam, C.C. Water transport through epoxy-based powder pipeline coatings. *Prog. Org. Coat.* **2022**, *168*, 106874. [[CrossRef](#)]
117. Ha, H.M.; Alfantazi, A. Effects of temperature and glass transition on the performance of polymer coatings on steels. In Proceedings of the 2014 10th International Pipeline Conference, Calgary, AB, Canada, 29 September–3 October 2014.

**Disclaimer/Publisher's Note:** The statements, opinions and data contained in all publications are solely those of the individual author(s) and contributor(s) and not of MDPI and/or the editor(s). MDPI and/or the editor(s) disclaim responsibility for any injury to people or property resulting from any ideas, methods, instructions or products referred to in the content.